Geological Journal

WILEY

SPECIAL ISSUE Continents

RESEARCH ARTICLE OPEN ACCESS

Identification of Multiple Thermal Events in High-Grade Metacarbonate Rocks Using Carbon Isotope Thermometry: An Example From the Sør Rondane Mountains, East Antarctica

M. Satish-Kumar[1] | Sasidharan Kiran[1] | Fumiko Higashino[2] | Tetsuo Kawakami[2] | Tomokazu Hokada[3,4]

[1]Department of Geology, Faculty of Science, Niigata University, Niigata, Japan | [2]Department of Geology and Mineralogy, Graduate School of Science, Kyoto University, Kyoto, Japan | [3]National Institute of Polar Research, Tokyo, Japan | [4]Polar Science Program, Graduate Institute for Advanced Studies, SOKENDAI, Tokyo, Japan

Correspondence: M. Satish-Kumar (satish@geo.sc.niigata-u.ac.jp)

Received: 30 April 2024 | **Revised:** 22 October 2024 | **Accepted:** 30 October 2024

Handling Editor: C.-X. Yang

Funding: This work was supported by the Grants-in-Aid for Scientific Research (KAKENHI) of the Japan Society for the Promotion of Science (JSPS) Nos. JP15H05831, JP20KK0081, JP22H04932, JP21H01182.

Keywords: carbon isotope thermometry | graphite | retrograde metamorphism | Sør Rondane Mountains | UHT metamorphism

ABSTRACT

Nine metacarbonate layers from the regionally metamorphosed terrane of the Sør Rondane Mountains in the Eastern Dronning Maud Land in East Antarctica were examined in detail for constraining the thermal events using carbon isotope exchange between dolomite/calcite and graphite. Equilibrium carbon isotope fractionation between dolomite and graphite suggested peak metamorphic temperature conditions reaching up to 802°C ± 29°C were estimated at the Balchenfjella locality, where multiple samples from six thick layers of metacarbonate rocks were examined. However, some of the samples exhibit lower carbon isotope fractionation reflecting the possibility of ultrahigh-temperature metamorphic conditions, which is consistent with recent reports. Furthermore, several metacarbonate rock samples display large variations in $\delta^{13}C_{VPDB}$ values for graphite grains, despite dolomite and calcite showing homogeneous carbon and oxygen isotopic composition indicating signatures of retrograde metamorphism and fluid infiltration events. Detailed textural observation suggested alteration of $\delta^{13}C_{VPDB}$ values of graphite during retrograde metamorphism might have resulted due to the overgrowth of graphite crystals by the infiltration of low $\delta^{13}C_{VPDB}$-bearing fluids, the extent of alteration being a direct function of the fluid–rock ratio. Field evidence indicates the presence of carbonate veins cutting across the metacarbonate rocks suggesting that carbon isotope thermometry can also be utilised to understand the effect of external fluid infiltration. At Perlebandet locality the metamorphic temperature conditions were estimated to be around 915°C, whereas those from Tanngarden and Menipa gave lower temperature estimates. Detailed textural analysis of graphite in combination with isotopic composition provided clear evidence for retrograde events. Thus, our results provide tight constraints of peak and post-peak metamorphic temperature conditions and a regional thermal structure for the Sør Rondane Mountains and further testify the usefulness of carbon isotope thermometry in polymetamorphic terrains.

1 | Introduction

Accurate estimation of peak metamorphic conditions is important in constraining the heat flow regimes and tectonic models of orogenic belts. In particular, terranes that experienced high- to ultrahigh-temperature (UHT) metamorphism provide signs for more than average heat flow from mantle and/or internal heat production in the continental lower crust. Peak metamorphic temperature conditions of >900°C have been reported in deep crustal rocks from more than 60 localities worldwide and these rocks have diagnostic mineral assemblages such as sapphirine + quartz and orthopyroxene + sillimanite + quartz (Harley 1998, 2008, 2021; Brown 2006, 2007; Kelsey 2008; Durgalakshmi et al. 2021). One of the characteristic feature of the East African-Antarctic Orogeny (EAAO) is the predominance of high to ultrahigh-temperature metamorphism, especially in southern Madagascar, southern India, Sri Lanka and East Antarctic sector where temperatures of >900°C of peak metamorphism is widely reported (e.g., Sajeev, Osanai, and Santosh 2004; Sajeev and Osanai 2004; Tsunogae and Santosh 2006; Yoshimura, Motoyoshi, and Miyamoto 2008; Jöns and Schenk 2011; Osanai et al. 2016a, 2016b; Durgalakshmi et al. 2021). Preservation and identification of high-temperature metamorphism and their post-peak metamorphic evolution are critical in determining how far the deep continental crust has withstood solid-state conditions, which in turn reflects the rheological properties and stability of the continental crust. Apart from the rare mineral assemblages, recent advances in temperature estimates using trace element based thermometries, such as Zr-in-rutile, Ti-in-quartz and Ti-in-zircon, in addition to ternary-feldspar thermometry can also help in the identification of peak metamorphic temperature conditions (e.g., Harley 2021; Higashino and Kawakami 2022; Suzuki and Kawakami 2019).

An independent way of recognition of peak metamorphic temperature conditions is the application of carbon isotope thermometry. The uniqueness of this method is the utilisation of carbon isotope exchange between two carbon-bearing minerals, carbonate and graphite (e.g., Bottinga 1969; Valley and O'Neil 1981; Wada and Suzuki 1983). The inertness of graphite to retrograde isotope exchange is considered as merit in using this thermometry in a large range of temperature conditions prevailing in the continental crust, even up to high- to ultrahigh-temperature metamorphic terrains (e.g., Satish-Kumar 2000; Satish-Kumar, Wada, and Santosh 2002). Carbon isotope thermometry has been successfully used to estimate the peak metamorphic temperatures in amphibolite to granulite facies metacarbonate rocks from several terrains across the globe (e.g., Valley and O'Neil 1981; Wada and Suzuki 1983; Morikiyo 1984; Dunn and Valley 1992; Morrison and Barth 1993; Kitchen and Valley 1995; Satish-Kumar, Wada, and Santosh 2002). This thermometry is based on the carbon isotope exchange between carbonate (calcite or dolomite) and graphite during prograde metamorphism, accompanied by recrystallisation of carbonate minerals and graphitisation of organic material trapped in carbonate sediments (Bottinga 1969; Valley and O'Neil 1981; Wada and Suzuki 1983). Pioneering empirical studies have suggested that equilibrium carbon isotope fractionation can be achieved above 400°C (Wada and Suzuki 1983), whereas experimental studies proved that carbon isotope exchange between carbonate and graphite is an irreversible process (Scheele and Hoefs 1992; Dienes and Eggler 2009). In addition, carbon isotope exchange can be estimated using theoretical methods as well (Chacko et al. 1991; Polyakov and Kharlashina 1995). Carbonate-dominated metamorphic rocks containing minor amounts of graphite are best suited for carbon isotope thermometry mainly due to the refractory nature of graphite, abundance of carbonate phase which possess fast diffusion of carbon and the absence of a third carbon-bearing phase (Dunn and Valley 1992; Satish-Kumar, Wada, and Santosh 2002). However, some previous studies have pointed out that if retrogression is accompanied by carbon-bearing fluid infiltration events, equilibrium fractionations can be disturbed to give erroneous temperature estimates and careful textural observation and grain-scale carbon isotope measurements can identify such disequilibrium isotope values (e.g., Satish-Kumar, Wada, and Santosh 2002; Satish-Kumar et al. 2011; Kiran et al. 2022).

Metacarbonate rocks are common in the Sør Rondane Mountains (SRM), East Antarctica (Osanai et al. 1992, 2013; Otsuji et al. 2013). This terrain is an integral part of the EAAO that formed during the collision orogeny between East and West Gondwana in the Neoproterozoic to Cambrian (Osanai et al. 2013; Satish-Kumar et al. 2013; Hokada, Satish-Kumar, and Kawakami 2024). Previous studies have suggested that this region has been extensively affected by pervasive retrograde Cl-rich hydrous fluid infiltrations, which resulted in the resetting of peak metamorphic mineral assemblages to a large extent (e.g., Higashino et al. 2013a; Kawakami et al. 2017; Uno, Okamoto, and Tsuchiya 2017; Higashino et al. 2019a, 2019b; Higashino et al. 2023b). Despite such regional-scale retrograde hydration, Higashino and Kawakami (2022) recently reported signatures of UHT conditions from the Balchenfjella locality of the SRM using ternary feldspar thermometry. Therefore, it is imperative to conduct a detailed investigation on the extent of high-temperature metamorphism. The present study reports the regional peak metamorphic temperature conditions at the SRM using carbon isotope thermometry in metacarbonate rocks. The results extend our understanding of peak and retrograde metamorphic conditions and discuss the potential application of carbon isotope thermometry in the identification of multiple thermal events in terranes affected by retrograde fluid infiltration events.

2 | Geological Background

The SRM belongs to the Meso- to Neoproterozoic collisional orogenic belt in the Eastern Dronning Maud Land, East Antarctica (Figure 1). This region comprises greenschist to granulite facies metamorphic rocks in association with various types of igneous rocks (Shiraishi et al. 1991; Asami et al. 1992). Geological studies carried out by the Japanese Antarctic Research Expeditions recognised two distinct terranes based on metamorphic grade, named the Northeastern (NE) and the Southwestern (SW) terranes separated by a high strain zone called the Sør Rondane Suture (SRS; Osanai et al. 1992). Recent geological and geochronological studies have led several researchers to consider that the Main Tectonic Boundary (MTB) is an important collision tectonic boundary (Figure 1; Osanai et al. 2013; Grantham et al. 2013;

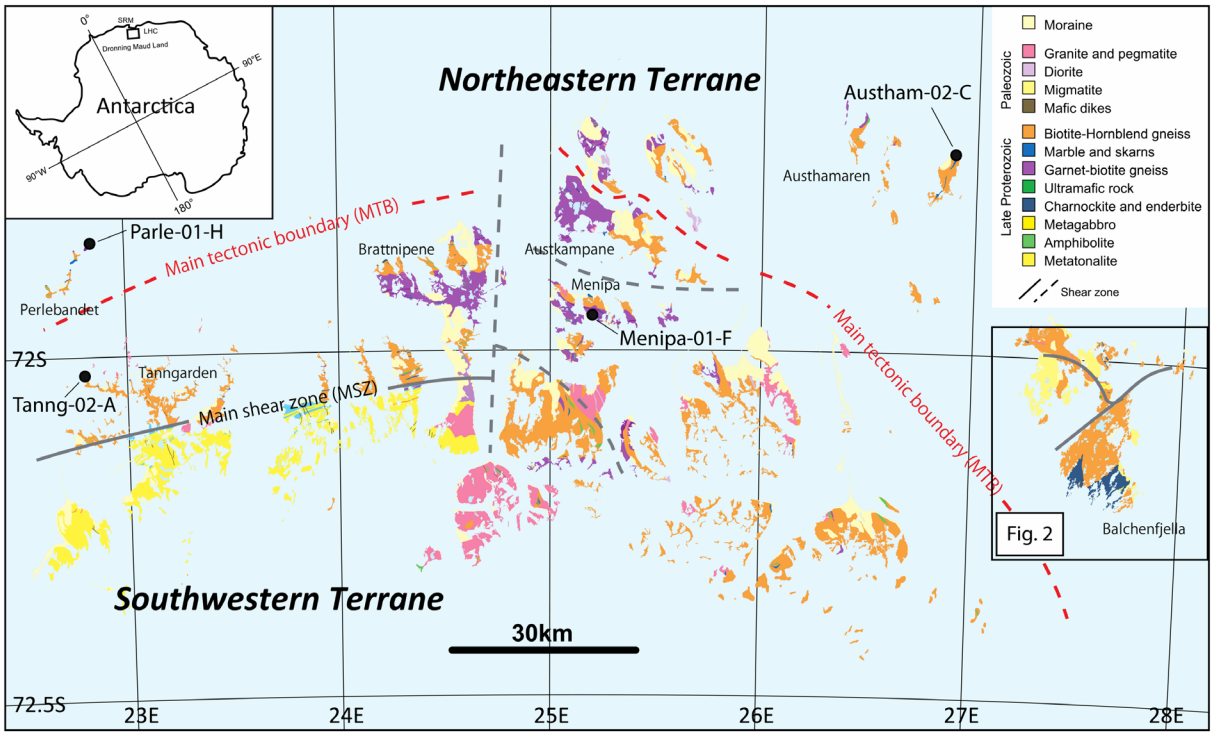

FIGURE 1 | Simplified geological map of Sør Rondane Mountains, East Antarctica after Shiraishi et al. (1997).

Mieth et al. 2014). The collision between the two terranes resulted in the thrusting of the NE terrane over the SW terrain at around 650–600 Ma and subsequent hydration and mylonitisation (Osanai et al. 2013; Adachi et al. 2023). The SRM has gained attention in understanding large-scale tectonics in the Gondwana assembly and the role of MTB in the tectonic evolution of this region is being reassessed by several recent studies focusing on pressure–temperature-deformation-time (*P–T-D-t*) evolution of rock units across the boundary (e.g., Osanai et al. 2013; Grantham et al. 2013; Kawakami et al. 2017; Tsubokawa et al. 2017; Ruppel et al. 2021; Hokada et al. 2022; Hokada, Satish-Kumar, and Kawakami 2024; Tsukada et al. 2023; Higashino et al. 2023a, 2023b).

Contrasting metamorphic *P–T* evolutions are recorded in NE and SW terranes across the MTB. The NE terrane records granulite facies conditions in general with a clockwise *P–T* path and the peak conditions were attained during 650–600 Ma (Shiraishi et al. 2008; Adachi et al. 2013a, 2013b; Grantham et al. 2013; Higashino et al. 2013a; Hokada et al. 2013, 2022; Hokada, Satish-Kumar, and Kawakami 2024). Detrital zircons older than 1200 Ma are common here (Kitano et al. 2016). In contrast, the SW Terrane records granulite to amphibolite facies conditions and a counterclockwise *P–T* path at 650–580 Ma (Shiraishi et al. 2008; Adachi et al. 2013a, 2013b; Nakano et al. 2013; Kawakami et al. 2017). The SW terrane is devoid of detrital zircon populations older than 1200 Ma (Kitano et al. 2016). However, some areas in the SW terrane have been found to show hair-pin to clockwise *P–T* path (Tsubokawa et al. 2017; Kawakami et al. 2022). Additionally, several stages of garnet-forming metamorphisms are reported from the entire SRM, potentially suggesting polymetamorphism in the SRM (Higashino et al. 2023a). Peak metamorphic conditions have been reported from several localities in the SRM and are compiled in Table 1. For example, the Balchenfjella region, which is a major outcrop examined in this study (Figure 2), has experienced a peak metamorphism of ~850°C, 1.1 GPa and retrograde metamorphism at ~540°C, 0.5 GPa (Table 1; Grantham et al. 2013; Higashino et al. 2013a, 2013b). Furthermore, Grantham et al. (2013) have reported the age relations of meta-igneous rocks from Austhamaren locality and suggested that the rocks have experienced metamorphism at >900°C at depths equivalent to >1.2 GPa at ~635 Ma. At the Menipa locality, while the prograde metamorphic *P–T* conditions are not constrained well, the peak metamorphic conditions of pelitic gneisses are estimated as ~1.0 GPa, ~800°C with a clockwise *P–T* path by Kawakami et al. (2022) (Table 1).

Granitoids of varying generations have been reported, the most prominent one is the ~640–600 Ma Dufek Granite, in addition to ~580–540 Ma leucogranites, pegmatites and minette and ~530–500 Ma granites (Kamei et al. 2013; Owada et al. 2010; Wang et al. 2020; Yuhara et al. 2023). Post-kinematic mafic dikes represent the youngest intrusions in the area (Owada et al. 2008).

The thick sequence of metasedimentary rocks is supposed to have been deposited in the Mozambique Ocean which existed between East and West Gondwana, prior to the orogenesis. Metacarbonate rocks often help in approximating a window of depositional ages (e.g., Halverson et al. 2005; Satish-Kumar et al. 2021). Otsuji et al. (2013) reported Tonian to Cryogenian (880–790 Ma) depositional ages of carbonate rocks in the SRM. Furthermore, geochemical and multielement isotopic studies indicated contrasting depositional environments depicted by an oceanic island arc system in the SW terrane, whereas the carbonate rocks in the NE terrane were supposed to have been deposited surrounding a matured craton (Otsuji et al. 2016).

TABLE 1 | Compilation of metamorphic conditions of the four localities investigated in this study.

Locality	*T* (°C)	Pressure (GPa)	Notes	Methods	Reference
Perlebandet	768–840	0.8–1.0	Peak	Zr-in-rutile thermometry, GASP geobarometry	Kawakami et al. (2017)
	~550	~0.4	Retrograde	Aluminosilicate triple point (microstructural constraint)	Kawakami et al. (2017)
	800–900	0.93-1.1	Peak	Ternary feldspar thermometry, GASP geobarometry	Higashino et al. (2023)
	590–645	0.24–0.35	Garnet breakdown	Grt-Bt geothermometry, GASP geobarometry, GBPQ geobarometry	Higashino et al. (2023)
	450–530	<0.45	Cl-bearing fluid infiltration	Two-feldspar thermometry, andalusite stability field	Higashino et al. (2023)
Tanngarden	~800	~0.7	Peak	Petrogenetic grid for the NaKFMASH system	Kawakami et al. (2021)
	~750	~0.3	Retrograde	Petrogenetic grid for the NaKFMASH system	Kawakami et al. (2021)
Menipa	~800	~1.0	Peak	Zr-in-rutile thermometry, coexistence of sillimanite and kyanite	Kawakami et al. (2022)
	~610	~0.38	Retrograde	Grt-Bt geothermometry, GASP geobarometry	Kawakami et al. (2022)
	~540	~0.29	Retrograde2 (finer grain)	Grt-Bt geothermometry, GASP geobarometry	Kawakami et al. (2022)
Balchenfjella (Gropeheia)	~850	~1.1	Peak	Grt-Bt geothermometry, GASP geobarometry	Higashino et al. (2013)
	~540	~0.5	Retrograde	Grt-Bt geothermometry, GASP geobarometry	Higashino et al. (2013)
	~900–1000	>1.2	Peak	Thermocalc	Grantham et al. (2013)
	700–850	0.7–1.0	Retrograde	Intersections of various reactions in five samples	Grantham et al. (2013)

Note: Note that only broad estimates of P–T conditions are reported from Austhamaren in Grantham et al. (2013).

2.1 | Metacarbonate Rocks From the Sør Rondane Mountains

In this study, a total of 24 metacarbonate samples from five different localities in the SRM were investigated in detail (Figure 1). The samples were collected during the geological field survey in the 51st Japanese Antarctic Research Expedition (JARE-51, 2010–2011, Tsuchiya et al. 2012). The metacarbonate layers occur as conformable units associated with metasedimentary and meta-igneous gneisses. The thickness of the layers varies from several decimetres to over 10 m, within which alternate pure and impure layers occur parallel to the regional trend of the major deformation. At some localities, skarn layers are developed between metacarbonate and gneisses. Calc-silicate minerals such as olivine, spinel, clinohumite, phlogopite, diopside and tremolite are commonly observed in the skarn layers.

Five major outcrops within the SRM, namely, Balchenfjella, Austhamaren, Menipa, Perlebandet and Tanngarden (Figure 1), were considered in detail because of the ubiquitous presence of carbonate—graphite association. Although metacarbonate rocks occur in several other localities (Otsuji et al. 2013), they are devoid of graphite and hence not considered here. Multiple samples were collected across the layering to verify the interaction with adjoining lithological units. Field relations of metacarbonate rocks from each region are presented in detail by Otsuji et al. (2013) and salient features are described below, including their mineralogical characteristics.

The Balchenfjella locality in the NE terrane is separated by the large Byrdbreen glacier from other regions in the SRM. Metasedimentary and meta-igneous and intrusive bodies are found in this region (Figure 2; Asami, Grew, and Makimoto 1990, 2007). Metapelitic rocks, metamorphosed mafic and ultramafic

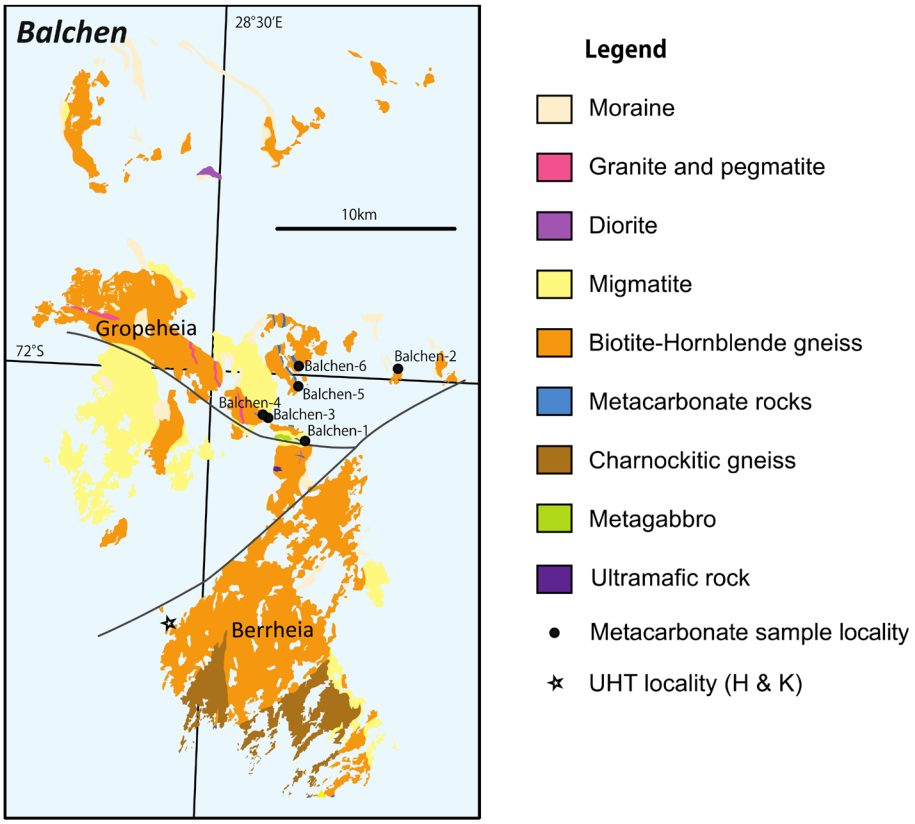

FIGURE 2 | Geological map of Balchenfjella region (after Asami et al. 1991; Asami, Grew, and Makimoto 2007; Ishikawa et al. 2013) showing the metacarbonate sampling localities. The locality where UHT conditions were reported is also shown (Higashino and Kawakami 2022).

rocks, and metacarbonate rocks are common here (Figure 2). Out of the nine layers that were sampled in the region, six layers contain graphite. These layers occur as conformable thick units with adjoining pelitic gneisses (Figure 3A,D). Thickness varies between the layers, the thinnest layer was about 20 cm in thickness whereas the thickest one (Balchen-5, Figure 3A) is about 10 m. Alternating calc-silicate mineral-bearing layers and carbonate-rich layers are observed (Figure 3B,C). Calc-silicate-bearing layers contain forsterite, diopside phlogopite, and spinel, whereas the carbonate-rich layers are predominated by dolomite, both layers having accessory amounts of graphite. The contact zones with surrounding pelitic rock units have thin zones of skarn formation (Figure 3D) and contain more calc-silicate minerals than the interior portions of the layers. Fracturing and late-stage veining with secondary alterations and formation of serpentine are observed in some of the layers, where both layer parallel veins (Figure 3C) as well as cross-cutting veins are observed (Figure 3E). The post-tectonic veining by granitic melts criss-crossing metacarbonate rocks is also observed in this region (Figure 3F), which is related to larger-scale granitic intrusive bodies in the region (e.g., Uno, Okamoto, and Tsuchiya 2017). Altogether 18 samples, collected from 6 layers from Balchenfjella locality were examined (Table 2).

Austhamaren is located in the north of NE terrane where several nunataks of granulite facies rocks are exposed (Figure 1). A thick metacarbonate layer of more than 5 m thickness is found interlayered with garnet-biotite-hornblende gneiss in the eastern part of the nunatak. The major rock units in this area are garnet-biotite-hornblende gneisses and a meta-igneous complex. The metacarbonate layer occurs ~2 km east of the meta-igneous complex reported by Grantham et al. (2013). Samples collected from this region are dolomite-rich with accessory amounts of graphite. Three samples were considered, two of which (Austham-2C and 2F) were collected from the central part of the layer, whereas Austham-2A is near the contact with hornblende-biotite gneiss. Minor amounts of forsterite and spinel are present in sample Austham-2A (Table 2).

Perlebandet is located in the western region of the SRM (Figure 1), where granulite facies garnet-biotite gneiss, garnet-sillimanite-biotite gneiss, hornblende-biotite gneiss, pyroxene granulite, orthopyroxene-bearing amphibolite, and metacarbonate rocks are exposed (Shiraishi et al. 1997; Kawakami et al. 2017). Although sillimanite is commonly found here, retrograde andalusite and kyanite are also reported (Kawakami et al. 2017). A recent study by Higashino et al. (2023b) suggested multiple generations of Cl-rich fluid activity, possibly related to granodiorite intrusion beneath the metamorphic rocks. Three metacarbonate layers occur in the Perlebandet locality from which one layer contains carbonate-graphite association was selected for this study, where skarn formation is observed in contact with metapelitic rocks (Figure 3G). One of the layers in this region contains clinohumite-bearing assemblage, whereas the other two layers are mostly pure dolomitic with accessory amounts of phlogopite (Table 2).

The metacarbonate layer studied from the east of Menipa locality in the central SRM was associated with sillimanite-bearing pelitic gneisses. This outcrop has received attention because of

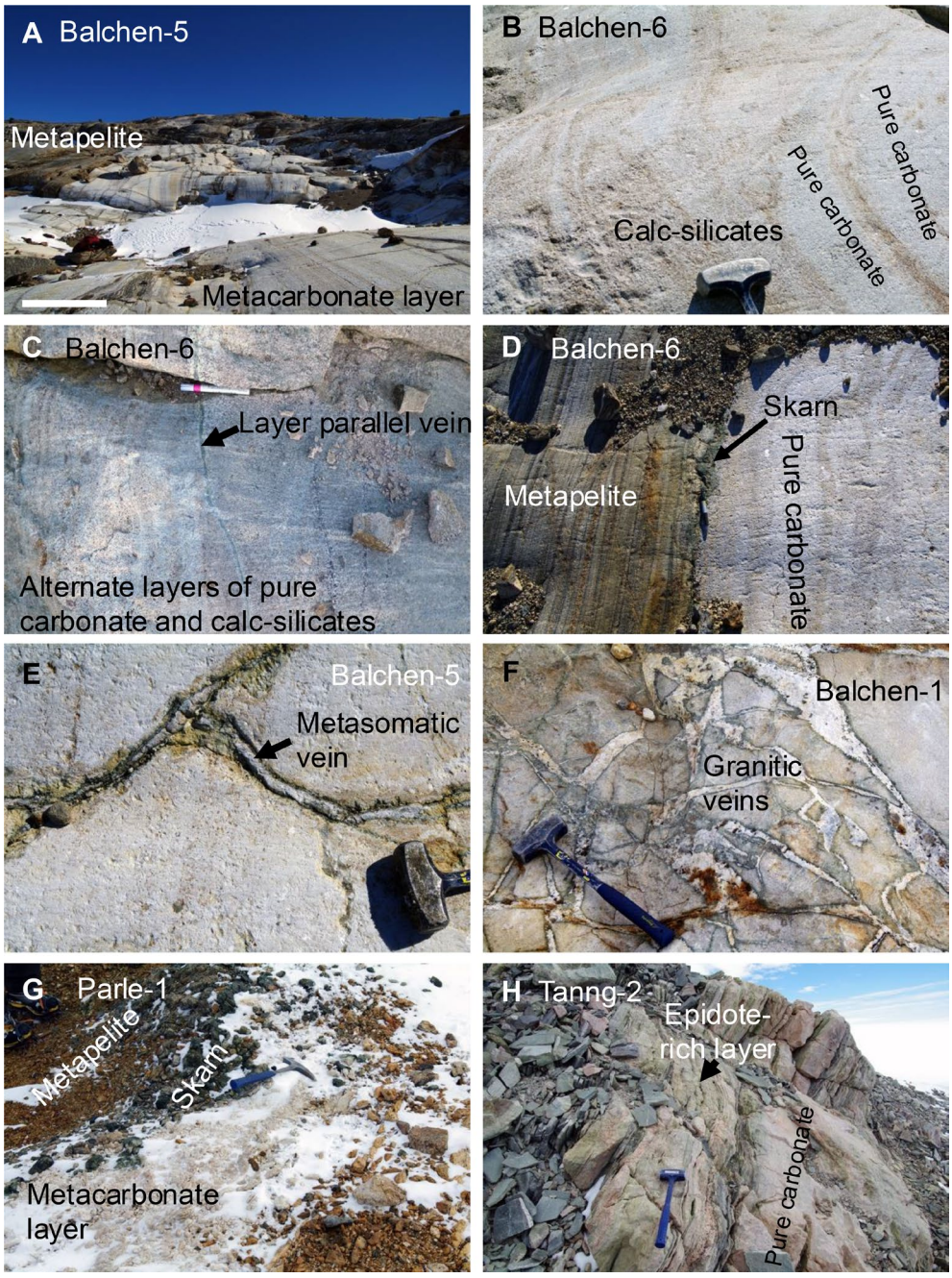

FIGURE 3 | Field occurrence of metacarbonate rocks in the Sør Rondane Mountains. (A) 30 m thick layer of metacarbonate rock from Balchen 5 locality (see Figure 2). (B, C) Alternating layers of carbonate-rich and silicate-rich metacarbonate rock at Balchenfjella. (D) Contact zone of metacarbonate layer with metapelite showing a thin layer of skarn formation. (E and F) Cross-cutting veins traversing metacarbonate layers at Balchenfjella. (G) Metacarbonate occurrence at Perlebandet showing the formation of skarn at the contact zone. (H) Metacarbonate occurrence at Tanngarden locality showing pinkish calcite-rich metacarbonate, with epidote-bearing layers formed during retrograde metamorphism.

the rare occurrence of V-bearing grossular garnet associated with graphitic schists (Osanai et al. 1990). Several thin metacarbonate layers are found intercalated with graphite-rich pelitic layers and some of these layers contain semiprecious varieties of ruby and sapphire (Table 2).

Tanngarden locality is situated in the SW terrane and dominated by meta-tonalitic rocks towards the south and schists and gneisses towards the north (Figure 1). A detailed estimate of *P–T* condition is lacking, however, based on mineral assemblages amphibolite facies condition is reported here (Osanai et al. 1992). Metacarbonate rocks occur here as thin layers associated with garnet-biotite gneiss or within the metatonalite rocks. Otsuji et al. (2013) studied metacarbonate rocks from Tanngarden, the eastern Vikinghogda, Teltet and Lunckeryggen. The metacarbonate layer at Lunkeryggen is composed of pink-coloured calcite and includes graphite flakes, whereas other layers are dolomite-rich with minor amounts of phlogopite and diopside (Table 2). In addition to the primary minerals, extensive retrograde formation of epidote is observed (Figure 3H).

TABLE 2 | List of metacarbonate rock sample studies from the Sør Rondane Mountains with mineral assemblages and grain size.

Serial no.	Locality	Sample code	Sample number	Latitude S	Longitude E	Carbonate mineral	Grain size (mm)	Graphite size (mm)	Graphite texture	Other silicate phases
1	Perlebandet	Parle-1H	20091130-01-H	71.87	22.76	Dolomite	2–15	< 0.5	Polygonal, highly reflecting	
2	Balchenfjella-1	Balchen-1A	20100115-02-A	72.04	27.65	Dolomite	1.2	< 2.0	Polygonal, highly reflecting	
3	Balchenfjella-1	Balchen-1B	20100115-02-B			Dolomite	1.0	< 1.2	Polygonal, highly reflecting	
4	Balchenfjella-1	Balchen-1C	20100115-02-C			Dolomite	2.0	< 0.5	Polygonal, highly reflecting	
5	Balchenfjella-2	Balchen-2B	20100118-02-B	72.00	27.79	Dolomite	5.0	< 2.5	Polygonal, highly reflecting	Fo, Di, Sp, Phl
6	Balchenfjella-3	Balchen-3A	20100119-01-A	72.02	27.58	Dolomite	1–8	< 0.5	Polygonal, highly reflecting	Di, Phl
7	Balchenfjella-3	Balchen-3C	20100119-01-C			Dolomite	1–10	< 0.6	Polygonal, highly reflecting	Fo, Di, Sp, Phl
8	Balchenfjella-4	Balchen-4E	20100119-03-E	72.02	27.58	Dolomite	10.0	< 0.8	Polygonal, highly reflecting	
9	Balchenfjella-4	Balchen-4F	20100119-03-F			Dolomite	7.0	< 0.5	Polygonal, highly reflecting	
10	Balchenfjella-5	Balchen-5A	20100119-05-A	72.01	27.63	Dolomite	3.0	< 1.0	Polygonal with overgrowths	Fo, Phl
11	Balchenfjella-5	Balchen-5B	20100119-05-B			Dolomite	5.0	< 0.5	Polygonal, highly reflecting	Fo, Phl
12	Balchenfjella-5	Balchen-5C	20100119-05-C			Dolomite	3.0	< 0.8	Polygonal, highly reflecting	Fo, Di, Sp, Phl
13	Balchenfjella-5	Balchen-5D	20100119-05-D			Dolomite	1.0	< 2.0	Polygonal, highly reflecting	Fo, Spl, Phl
14	Balchenfjella-5	Balchen-5E	20100119-05-E			Dolomite	2–5	< 0.4	Polygonal, highly reflecting	Fo, Spl, Phl
15	Balchenfjella-5	Balchen-5F	20100119-05-F			Dolomite	4.0	< 0.5	Polygonal, highly reflecting	Fo, Phl
16	Balchenfjella-6	Balchen-6C	20100123-02-C	72.00	27.61	Dolomite	3.0	< 0.8	Polygonal, highly reflecting	Fo, Phl
17	Balchenfjella-6	Balchen-6D	20100123-02-D			Dolomite	1.0	< 0.5	Polygonal, highly reflecting	
18	Balchenfjella-6	Balchen-6E	20100123-02-E			Dolomite	2–5	< 1.5	Polygonal with overgrowths	Fo, Di, Sp, Phl
19	Balchenfjella-6	Balchen-6F	20100123-02-F			Dolomite	2.0	< 0.5	Polygonal with overgrowths	Fo, Di, Sp, Phl
20	Austhamaren	Austham-2A	20100124-02-A	71.71	26.88	Dolomite	5.0	< 1.2	Polygonal, highly reflecting	
21	Austhamaren	Austham-2C	20100124-02-C			Dolomite	8.0	< 2.5	Polygonal, highly reflecting	Sp
22	Austhamaren	Austham-2F	20100124-02-F			Dolomite	8.0	< 1.5	Polygonal, highly reflecting	
23	Tanngarden	Tanng-2A	20091127-02-A	72.12	24.39	Calcite	3.0	< 0.5	Polygonal, highly reflecting	Tr, Phl, Di
24	Menipa	Menipa-1F	20091213-01-F	71.96	25.23	Calcite	2.5	< 3.0	Irregular, rough surfaced	Sp, Cor

Abbreviations: Cor, corundum; Di, diopside; Fo, forsterite; Hum, humite; Phl, phlogopite; Sp, spinel; Tr, tremolite.

3 | Sample Descriptions

Twenty-four metacarbonate samples from localities containing graphite were selected for detailed isotope analyses. Localities from where the samples were collected, salient field relationship and mineralogical characteristics are compiled in Table 2.

3.1 | Macroscopic Observations

All samples were cut, polished and stained with alizarin red S in dilute HCl to distinguish between calcite and dolomite. We have selected samples with carbonate-rich layers, which are pure white to greyish to yellowish colour, that contain more than 90% of carbonate phases and minor occurrences of graphite (Figure 4). However, some samples, especially those near the contact with metapelitic rocks exhibit higher calc-silicate mineral abundance. There is a large variation in grain size of carbonate minerals from less than a millimetre (Figure 4A) to coarse-grained ones with several centimetres in diameter (Figure 4E,F). The coarse-grained samples sometimes display recrystallisation along grain boundaries. Furthermore, the proportion of calc-silicate minerals to carbonate minerals also varies, as observed in the polished slabs (Figure 4B,E,F). The major calc-silicate minerals in the Balchenfjella occurrence are olivine, diopside, phlogopite, and clinohumite with minor amounts of other phases such as spinel, apatite, and graphite (Figure 4A,B).

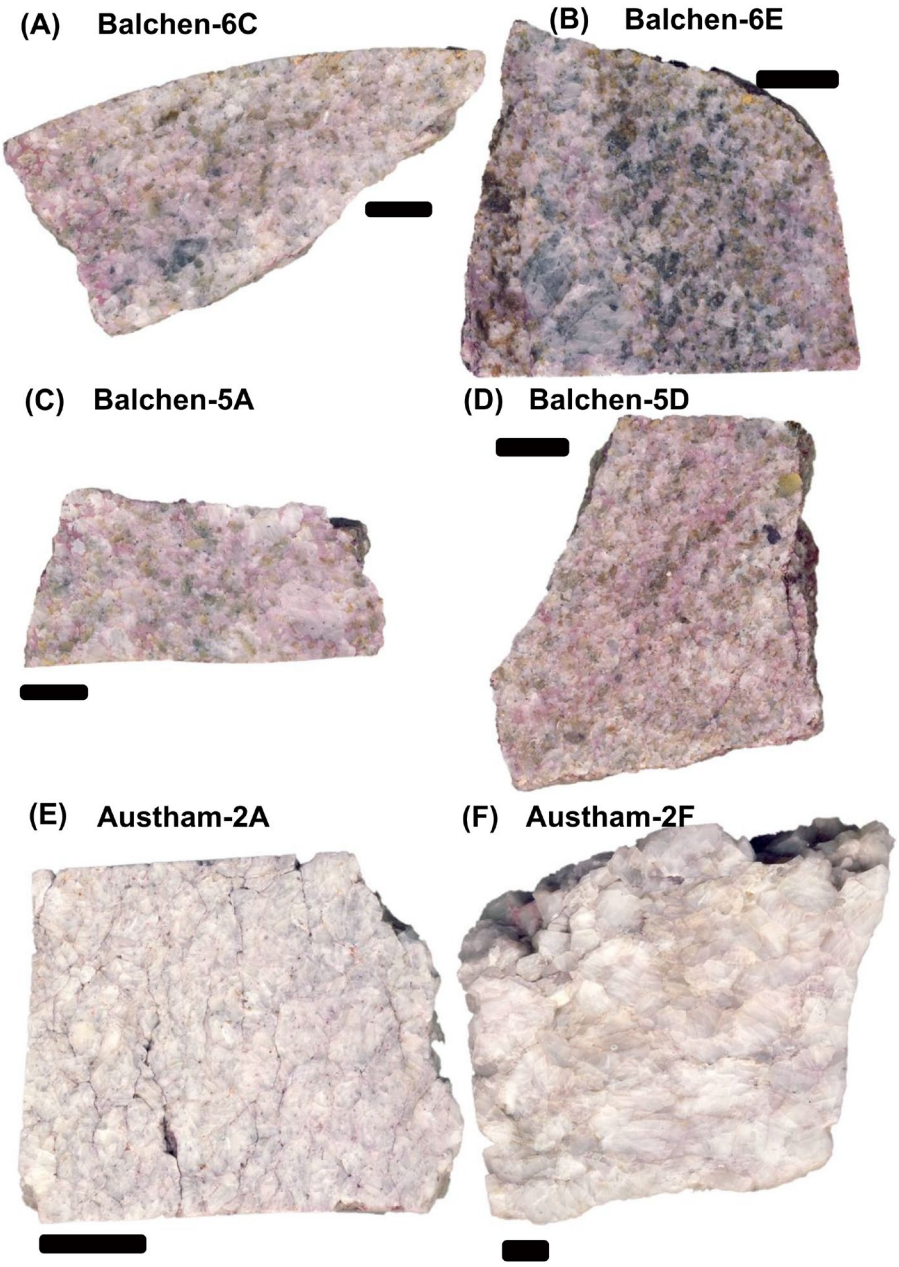

FIGURE 4 | Photographs of slabs of metacarbonate rocks showing the mineralogical variations observed in different metacarbonate rocks in the Sør Rondane Mountains. The slabs were stained using Alizarin-Red S for distinguishing between calcite (pink) and dolomite (unstained). Scale bars represent 1 cm.

3.2 | Microscopic Observations

Thin section petrography indicated that the calc-silicate minerals vary between samples, however in general forsterite, diopside, phlogopite and spinel are common (Figure 5A,B). Euhedral flakes of graphite are present in varying proportions (Figure 5C–F). Graphite flakes vary in size from fine-grained to more than a millimetre. They occur in grain boundaries between dolomite grains or as inclusions (Figure 5C). Association with silicate minerals such as forsterite and phlogopite are also observed (Figure 5D); however, these flakes were not considered in the isotopic study because previous studies have reported that armoring of silicate grains can cause isotopic disequilibrium (Arita and Wada 1990; Dunn 2005). At the Austhamaren locality, euhedral graphite grains are completely embedded in coarse crystals of dolomite which shows the twinning characteristic of high-temperature conditions (Figure 5E,F). In order to avoid any retrograde isotope exchange with secondary carbonate phases, care was taken to choose homogeneous coarse-grained dolomite/calcite grains for isotopic analysis, although at high-temperature conditions calcite-dolomite fractionation is relatively small (Sheppard and Schwarz 1970).

3.3 | Textural Characteristics of Graphite

Reflected light microscope observations of independent graphite flakes obtained from the dissolution of carbonate in HCl were carried out. The majority of the graphite flakes in the samples studied possess euhedral shapes. The textural features of graphite flakes were observed under a scanning electron microscope in detail for representative samples. The graphite grains in two samples from the Balchenfjella locality (Balchen-5A and Balchen-6E) that displayed large heterogeneity in carbon isotope compositions (Table 3) displayed crystalline hexagonal to semi-hexagonal forms with smooth high reflecting surface (Figure 6A). The peculiarity of the grains was the prominent overgrowth features with polygonal small crystals forming on the surface of pre-existing euhedral large grains (Figure 6C,D). Occasionally, regular graphite crystals with partially rough and dull surface were also observed. In contrast, the graphite grains in an isotopically homogenous sample (Balchen 6C) showed polygonal crystal shapes and did not show any signs of overgrowth features (Figure 6B,E,F). Graphite grains from the Menipa locality showed rough surface features with dull reflection and overgrowth textures (Figure 6G). At the Tangarden locality, the graphite grains are highly corroded, fragile and porous with dull reflection (Figure 6H).

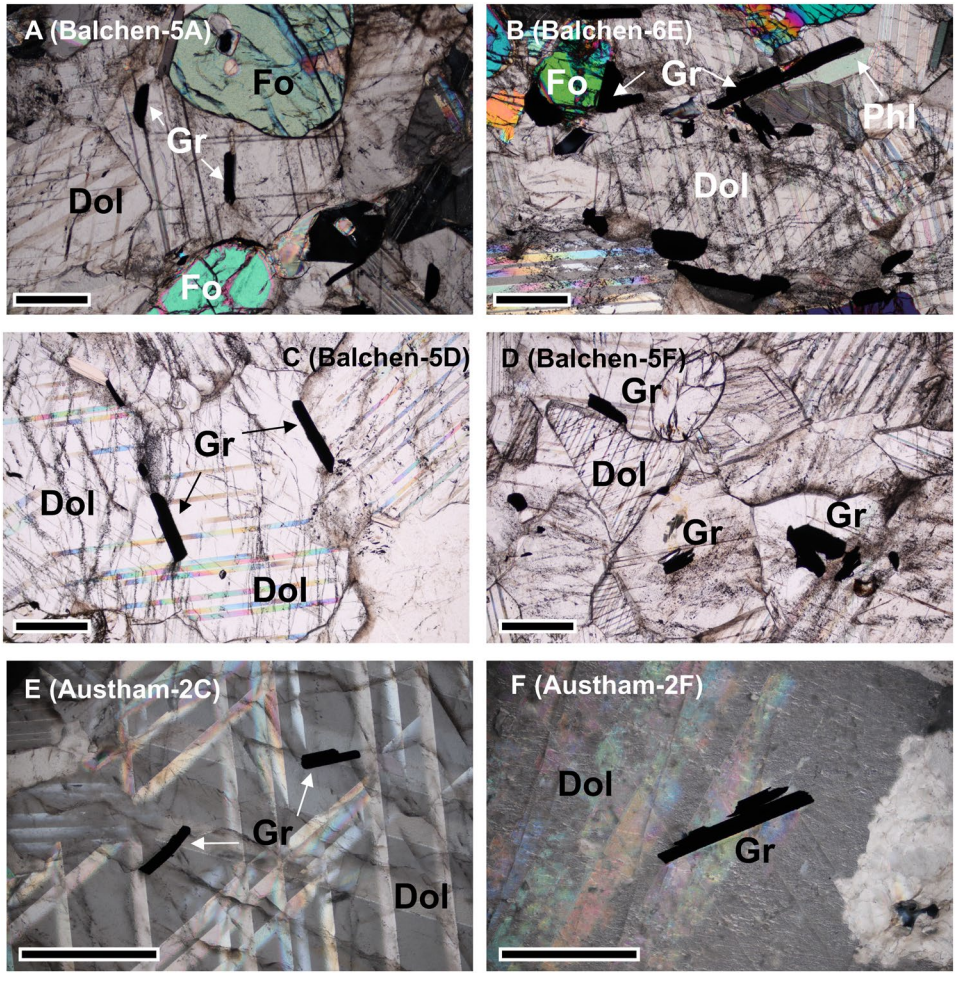

FIGURE 5 | Representative photomicrographs of metacarbonate rocks showing graphite embedded in equigranular dolomite/calcite from various localities in the Sør Rondane Mountains. A, B, E and F are in crossed polars, C and D are in plane-polarised light. Mineral abbreviations are Dol: dolomite, Fo: forsterite, Phl: phlogopite and Gr: graphite. Scale bar represents 1 mm.

TABLE 3 | Carbon and oxygen isotopic composition of carbonates and carbon isotopic composition of graphite with average fractionation and temperature estimates.

				Calcite						Graphite			Fractionation and temperature estimates				
Sample code	Sample number	Mineral	Textural position of analysis	$\delta^{13}C_{VPDB}$	$\delta^{18}O_{VSMOW}$	Average of core $\delta^{13}C_{VPDB}$ (‰)	1σ	Average of core $\delta^{18}O_{VSMOW}$ (‰)	1σ	$\delta^{13}C_{VPDB}$	Average of polygonal grains $\delta^{13}C_{VPDB}$	1σ	Δ Average carb − Average gr (‰)	1σ	Aver T (K & V)	+/−	Aver T (P & K @1 GPa)
Parle-1H	20091130-01-H	dol1	Whole grain	1.92	24.47	1.97	0.19	23.68	1.28				2.52	0.31	915	+81/−66	851
		dol2	Whole grain	2.18	24.37								2.83		849	66	
		dol3	Whole grain	1.80	22.21								2.21		996	81	
		gr1	Polygonal							−0.37	−0.55	0.12					
		gr2	Polygonal							−0.65							
		gr3	Polygonal							−0.65							
		gr4	Polygonal							−0.61							
		gr5	Polygonal							−0.47							
Balchen-1A	20100115-02-A	dol1	Core	0.75	22.21	0.76	0.01	22.17	0.06				3.16	0.19	788	+34/−30	725
		dol2	Core	0.76	22.12								3.35		758	30	
		gr1	Polygonal							−2.24	−2.40	0.18	2.97		822	34	
		gr2	Polygonal							−2.60							
		gr3	Polygonal							−2.36							
Balchen-1B	20100115-02-B	cc1	Multiple grains	0.17	22.82	0.45	0.20	22.40	0.38				2.80	0.55	854	+131/−96	790
		cc2	Multiple grains	0.32	22.73								3.35		758	96	
		cc3	Multiple grains	0.51	21.89								2.25		985	131	
		cc4	Multiple grains	0.63	22.21												
		cc5	Multiple grains	0.62	22.36												
		gr1	Polygonal							−2.32	−2.35	0.35					
		gr2	Polygonal							−2.84							
		gr3	Polygonal							−2.00							
		gr4	Polygonal							−2.24							

(Continues)

TABLE 3 | (Continued)

				Calcite						Graphite			Fractionation and temperature estimates				
Sample code	Sample number	Mineral	Textural position of analysis	$\delta^{13}C_{VPDB}$	$\delta^{18}O_{VSMOW}$	Average of core $\delta^{13}C_{VPDB}$ (‰)	1σ	Average of core $\delta^{18}O_{VSMOW}$ (‰)	1σ	$\delta^{13}C_{VPDB}$	Average of polygonal grains $\delta^{13}C_{VPDB}$	1σ	Δ Average carb – Average gr (‰)	1σ	Aver T (K & V)	+/−	Aver T (P & K @1 GPa)
Balchen-1C	20100115-02-C	dol1	Core	−0.93	23.12	−0.75	0.25	23.04	0.06				2.09	0.54	1032	+210/−142	786
		dol2	Core	−0.57	22.97								2.63		890	142	
		dol3	Recrystallised	0.68	23.03								1.55		1242	210	
		dol4	Recrystallised	0.74	23.03												
		gr1	Polygonal							−3.11	−2.84	0.29					
		gr2	Polygonal							−2.54							
		gr3	Polygonal							−2.86							
Balchen-2B	20100118-02-B	cc1	Recrystallised	0.93	13.14	0.32	0.04	14.06	1.01				2.36	0.21	955	+59/−51	812
		cc2	Recrystallised	1.07	13.29								2.57		904	51	
		cc3	Core	0.35	15.20								2.15		1014	59	
		cc4	Core	0.29	14.62												
		gr1	Polygonal							−1.88	−2.04	0.17					
		gr2	Polygonal							−2.22							
		gr3	Polygonal							−2.02							
Balchen-3A	20100119-01-A	dol1	Core	−2.26	20.40	−2.20	0.08	20.49	0.12				3.12	0.25	795	+46/−40	732
		dol2	Core	−2.14	20.57								3.37		755	40	
		gr1	Polygonal							−5.17	−5.32	0.17	2.87		841	46	
		gr2	Polygonal							−5.51							
		gr3	Polygonal							−5.28							
Balchen-3C	20100119-01-C	dol1	Core	0.30	25.78	0.22	0.12	25.33	0.64				2.97	1.07	822	+274/−156	759
		dol2	Core	0.13	24.88								4.04		666	156	
		gr1	Polygonal							−3.55	−2.76	0.95	1.90		1096	274	
		gr2	Polygonal							−1.71							
		gr3	Polygonal							−3.01							

(Continues)

TABLE 3 | (Continued)

				Calcite						Graphite			Fractionation and temperature estimates				
Sample code	Sample number	Mineral	Textural position of analysis	$\delta^{13}C_{VPDB}$	$\delta^{18}O_{VSMOW}$	Average of core $\delta^{13}C_{VPDB}$ (‰)	1σ	Average of core $\delta^{18}O_{VSMOW}$ (‰)	1σ	$\delta^{13}C_{VPDB}$	Average of polygonal grains $\delta^{13}C_{VPDB}$	1σ	Δ Average carb – Average gr (‰)	1σ	Aver T (K & V)	+/−	Aver T (P & K @1 GPa)
Balchen-4E	20100119-03-E	dol1	Core	−1.14	18.29	−0.91	0.17	19.49	0.94				3.20	0.31	782	+55/−48	719
		dol2	Core	−0.84	20.30								3.51		734	48	
		dol3	Core	−0.74	20.19								2.89		837	55	
		dol4	Core	−0.91	19.19												
		gr1	Polygonal							−4.03	−4.11	0.14					
		gr2	Polygonal							−4.03							
		gr3	Polygonal							−4.27							
Balchen-4F	20100119-03-F	dol1	Core	−0.92	20.35	−0.89	0.03	20.18	0.14				2.99	0.18	818	+34/−31	755
		dol2	Core	−0.86	20.10								3.17		787	31	
		dol3	Core	−0.90	20.10								2.81		852	34	
		gr1	Polygonal							−3.95	−3.88	0.15					
		gr2	Polygonal							−3.71							
		gr3	Polygonal							−3.98							
Balchen-5A	20100119-05-A	cc1	Fine recrystallised	−2.24	23.85	−3.14	0.39	23.45	0.72				3.43	0.49	746	+81/−66	475
		cc2	Fine recrystallised	−2.94	23.08								3.92		680	66	
		cc3	Fine recrystallised	−2.65	22.44								2.94		827	81	
		dol1	Core	−2.94	24.19												
		dol2	Core	−3.31	24.17												
		dol3	Core	−3.18	22.99												
		gr1	Polygonal							−6.53	−6.57	0.10					
		gr2	With overgrowth							−11.56							
		gr3	Polygonal							−6.46							
		gr4	Polygonal							−6.60							
		gr5	With overgrowth							−12.01							
		gr6	Polygonal							−6.70							

(Continues)

TABLE 3 | (Continued)

				Calcite						Graphite			Fractionation and temperature estimates				
Sample code	Sample number	Mineral	Textural position of analysis	$\delta^{13}C_{VPDB}$	$\delta^{18}O_{VSMOW}$	Average of core $\delta^{13}C_{VPDB}$ (‰)	1σ	Average of core $\delta^{18}O_{VSMOW}$ (‰)	1σ	$\delta^{13}C_{VPDB}$	Average of polygonal grains $\delta^{13}C_{VPDB}$	1σ	Δ Average carb – Average gr (‰)	1σ	Aver T (K & V)	+/−	Aver T (P & K @1 GPa)
Balchen-5B	20100119-05-B	dol1	Core	−1.58	23.77	−1.69	0.16	23.54	0.33				4.33	0.31	634	+34/−31	572
		dol2	Core	−1.80	23.30								4.64		603	31	
		gr1	Polygonal							−6.04	−6.02	0.15	4.02		668	34	
		gr2	Polygonal							−6.16							
		gr3	Polygonal							−5.87							
Balchen-5C	20100119-05-C	dol1	Core	−3.72	23.80	−3.43	0.25	23.36	0.77				3.13	0.43	793	+82/−66	714
		dol2	Core	−3.25	23.81								3.56		727	66	
		dol3	Core	−3.33	22.47								2.70		875	82	
		gr1	Polygonal							−6.69	−6.57	0.18					
		gr2	Polygonal							−6.44							
Balchen-5D	20100119-05-D	dol1	Core	−2.86	23.69	−2.86	0.04	23.70	0.06				3.38	0.18	753	+29/−26	690
		dol2	Core	−2.90	23.69								3.56		727	26	
		dol3	Core	−2.86	23.65								3.20		782	29	
		dol4	Core	−2.80	23.78												
		gr1	Polygonal							−6.13	−6.23	0.14					
		gr2	Polygonal							−6.33							
Balchen-5E	20100119-05-E	dol1		−1.60	25.19	−1.58	0.03	25.05	0.21				4.28	0.15	639	+16/−16	577
		dol2		−1.56	24.90								4.43		623	16	
		gr1	Polygonal							−5.94	−5.86	0.12	4.13		655	16	
		gr2	Polygonal							−5.77							
Balchen-5F	20100119-05-F	cc1	Core	−2.65	22.25	−2.79	0.20	22.29	0.05				3.03	0.50	811	+102/−80	748
		cc2	Core	−2.93	22.32								3.53		731	80	
		gr1	Polygonal							−5.68	−5.82	0.30	2.53		913	102	
		gr2	Polygonal							−5.61							
		gr3	Polygonal							−6.16							

(Continues)

TABLE 3 | (Continued)

				Calcite						Graphite			Fractionation and temperature estimates				
Sample code	Sample number	Mineral	Textural position of analysis	$\delta^{13}C_{VPDB}$	$\delta^{18}O_{VSMOW}$	Average of core $\delta^{13}C_{VPDB}$ (‰)	1σ	Average of core $\delta^{18}O_{VSMOW}$ (‰)	1σ	$\delta^{13}C_{VPDB}$	Average of polygonal grains $\delta^{13}C_{VPDB}$	1σ	Δ Average carb – Average gr (‰)	1σ	Aver T (K & V)	+/−	Aver T (P & K @1 GPa)
Balchen-6C	20100123-02-C	dol1	Core	−1.64	25.15	−1.80	0.22	25.16	0.01				4.32	0.35	635	+39/−35	573
		dol2	Multiple grains	−1.95	25.17								4.67		600	35	
		gr1	Polygonal							−6.18	−6.11	0.15	3.97		674	39	
		gr2	Polygonal							−6.06							
		gr3	Polygonal							−6.24							
		gr4	Polygonal							−6.21							
		gr5	Polygonal							−5.87							
Balchen-6D	20100123-02-D	dol1	Core	−1.09	25.20	−1.02	0.11	25.15	0.08				3.67	0.48	712	+71/−59	654
		dol2	Core	−0.94	25.09								4.15		653	59	
		gr1	Polygonal							−4.44	−4.69	0.37	3.19		783	71	
		gr2	Polygonal							−4.67							
		gr3	Polygonal							−4.23							
		gr4	Polygonal							−5.13							
		gr5	Polygonal							−4.97							
Balchen-6E	20100123-02-E	dol1	Multiple grains	−4.13	21.60	−3.88	0.36	21.71	0.22				6.57	3.74	463	+385/—	401
		dol2	Multiple grains	−4.24	21.56								10.31		—		
		dol3	Multiple grains	−3.63	22.04								2.83		848	385	
		dol4	Multiple grains	−3.51	21.64												
		gr1	With overgrowth							−9.16	−10.45	3.38					
		gr2	With overgrowth							−11.38							
		gr3	With overgrowth							−13.52							
		gr4	With overgrowth							−12.87							
		gr5	Polygonal							−4.26							
		gr6	With overgrowth							−11.51							

(Continues)

TABLE 3 | (Continued)

				Calcite						Graphite			Fractionation and temperature estimates				
Sample code	Sample number	Mineral	Textural position of analysis	$\delta^{13}C_{VPDB}$	$\delta^{18}O_{VSMOW}$	Average of core $\delta^{13}C_{VPDB}$ (‰)	1σ	Average of core $\delta^{18}O_{VSMOW}$ (‰)	1σ	$\delta^{13}C_{VPDB}$	Average of polygonal grains $\delta^{13}C_{VPDB}$	1σ	Δ Average carb − Average gr (‰)	1σ	Aver T (K & V)	+/−	Aver T (P & K @1 GPa)
Balchen-6F	20100123-02-F	dol1	Multiple grains	−5.47	20.91	−4.47	0.71	20.63	0.26				3.74	1.27	703	+224/−133	640
		dol2	Multiple grains	−4.98	20.74								5.01		570	133	
		dol3	Multiple grains	−4.03	20.21								2.47		927	224	
		dol4	Multiple grains	−3.90	20.59												
		dol5	Multiple grains	−3.96	20.68												
		gr1	Polygonal							−8.83	−8.21	0.56					
		gr2	Polygonal							−8.06							
		gr3	Polygonal							−7.74							
Austham-2A	20100124-02-A	dol1	Core	0.90	25.43	0.65	0.35	24.51	1.05				3.22	1.07	778	+236/−140	715
		dol2	Core	1.11	25.81								4.29		638	140	
		dol3	Rim	0.46	23.85								2.15		1014	236	
		dol4	Rim	0.52	24.12												
		dol5	Rim	0.26	23.36												
		gr1	Polygonal							−2.41	−2.57	0.72					
		gr2	Polygonal							−3.35							
		gr3	Polygonal							−1.94							
Austham-2C	20100124-02-C-1	dol1	Core	2.87	24.16	3.24	0.55	23.46	0.48				2.59	0.76	900	+221/−142	
		dol2	Core	2.94	24.23								3.35		758	142	
		dol3	Core	2.64	23.43								1.83		1121	221	
		dol4	Core	2.71	23.49												
		dol5	Core	2.75	23.02												
		gr1	Polygonal							0.66	0.65	0.21					
		gr2	Polygonal							0.76							
		gr3	Polygonal							1.06							
		gr4	Polygonal							1.17							
		gr5	Polygonal							0.84							

(Continues)

TABLE 3 | (Continued)

				Calcite						Graphite			Fractionation and temperature estimates				
Sample code	Sample number	Mineral	Textural position of analysis	$\delta^{13}C_{VPDB}$	$\delta^{18}O_{VSMOW}$	Average of core $\delta^{13}C_{VPDB}$ (‰)	1σ	Average of core $\delta^{18}O_{VSMOW}$ (‰)	1σ	$\delta^{13}C_{VPDB}$	Average of polygonal grains $\delta^{13}C_{VPDB}$	1σ	Δ Average carb – Average gr (‰)	1σ	Aver T (K & V)	+/−	Aver T (P & K @1 GPa)
In situ measurements	20100124-02-C-2																
	Dolomite-graphite Pair-1 (Figure 9E)	dol 6	In contact with gr	3.94	23.50	3.90	0.06	23.44	0.08				3.52		733		
		dol 7	5 mm away from gr	3.85	23.38												
		gr6	Polygonal							0.38							
	Dolomite-graphite Pair-2 (Figure 9F)	dol 8	In contact with gr	3.67	22.80	3.73	0.08	22.97	0.23				4.07		662		
		dol 9	5 mm away from gr	3.79	23.13												
		gr7	Polygonal							−0.34							
Austham-2F	20100124-02-F-1	dol1	Core	3.73	24.11	3.75	0.34	22.96	1.56				2.84	0.55	843	+131/−91	
		dol2	Core	3.18	20.22								3.39		752	91	
		dol3	Rim	2.38	17.79								2.29		974	131	
		dol4	Rim	1.74	22.54												
		dol5	Rim	1.67	21.58												
		gr1	Polygonal							1.07	0.92	0.22					
		gr2	Polygonal							1.02							
In situ measurements	20100124-02-F-2																
	Dolomite-graphite Pair-1 (Figure 9G)	dol6	In contact with gr	4.02	23.78	4.00	0.03	23.64	0.12				3.24		775		
		dol7	5 mm away from gr	4.00	23.61												
		dol8	2 cm away from gr	3.97	23.54												
		gr3	Polygonal							0.76							
	Dolomite-graphite Pair-2 (Figure 9H)	dol9	In contact with gr	3.79	22.97	3.84	0.06	23.14	0.24				3.18		785		
		dol10	5 mm away from gr	3.88	23.31												
		gr3	Polygonal							0.66							

(Continues)

TABLE 3 | (Continued)

				Calcite						Graphite			Fractionation and temperature estimates				
Sample code	Sample number	Mineral	Textural position of analysis	$\delta^{13}C_{VPDB}$	$\delta^{18}O_{VSMOW}$	Average of core $\delta^{13}C_{VPDB}$ (‰)	1σ	Average of core $\delta^{18}O_{VSMOW}$ (‰)	1σ	$\delta^{13}C_{VPDB}$	Average of polygonal grains $\delta^{13}C_{VPDB}$	1σ	Δ Average carb – Average gr (‰)	1σ	Aver T (K & V)	+/–	Aver T (P & K @1 GPa)
Tanng-2A	20091127-02-A	dol1	Multiple grains	−1.98	17.80	−1.53	0.42	17.46	2.73				6.45	0.60	470	+37/−32	408
		dol2	Multiple grains	−0.98	12.95								7.05		438	32	
		dol3	Multiple grains	−1.90	17.29								5.85		507	37	
		dol4	Multiple grains	−1.29	19.66												
		dol5	Multiple grains	−1.50	19.59												
		gr1	Dull corroded							−8.11	−7.98	0.18					
		gr2	Dull corroded							−7.85							
Menipa-1F	20091213-01-F	dol1	Multiple grains	3.00	22.04	3.18	0.24	22.68	1.02				4.98	0.44	572	+40/−34	511
		dol2	Multiple grains	3.08	22.15								5.42		538	34	
		dol3	Multiple grains	3.45	23.86								4.54		612	40	
		gr1	Dull corroded							−1.66	−1.80	0.20					
		gr2	Dull corroded							−1.94							

Abbreviations: K & V, Kitchen and Valley (1995); P & K, Polyakov and Kharlashina (1995).

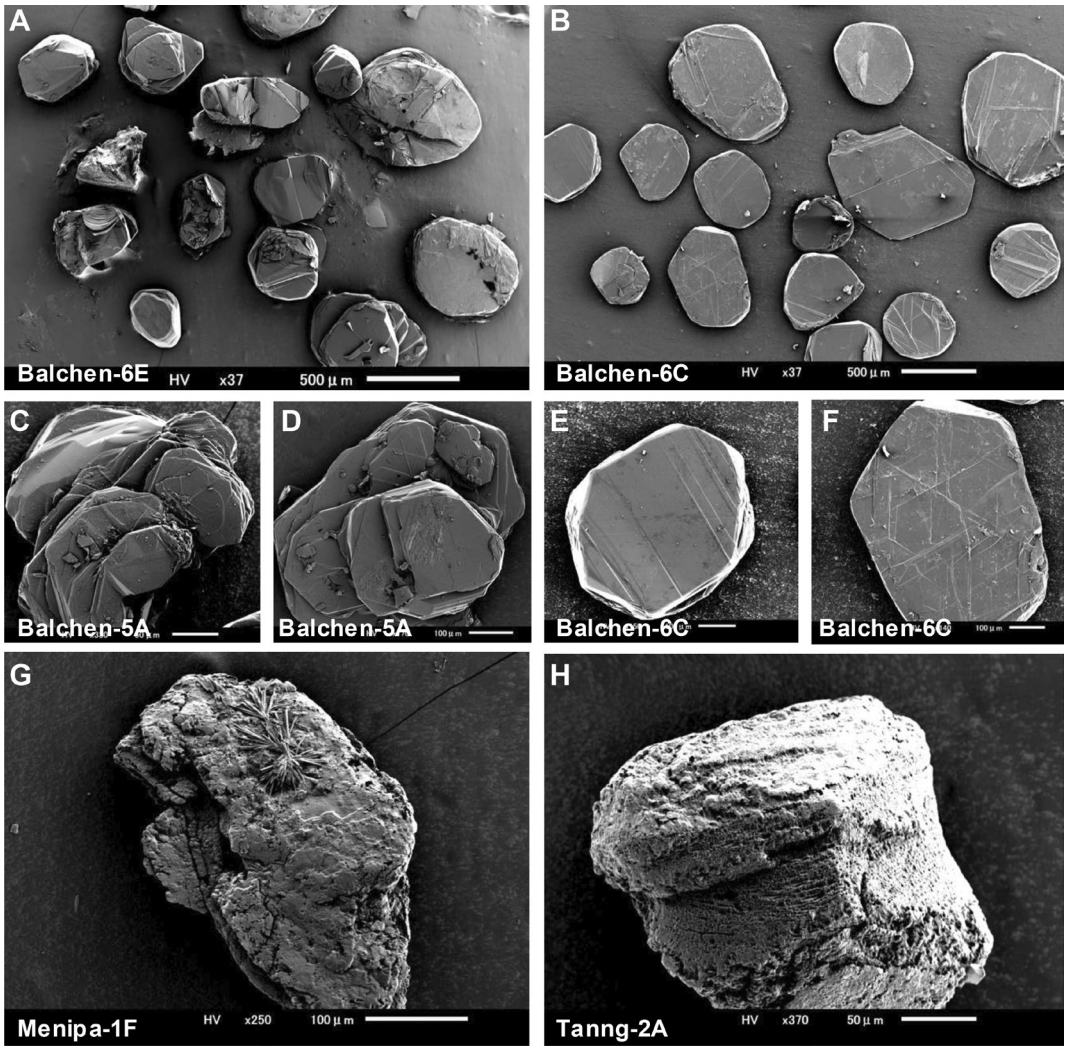

FIGURE 6 | Representative scanning electron microscope images of graphite crystals in samples from the Balhenfjella locality, which shows carbon isotopic heterogeneity (A) and homogeneity (B). (C, D). Graphite crystals show overgrowth of smaller crystal, plausibly during the retrograde overgrowth. (E, F). Euhedral polygonal crystal of graphite without overgrowth features. Such graphite crystals gave homogeneous isotope values, which are in equilibrium with carbonate. (G). Dull surface with overgrowth texture displayed by a graphite grain from the Menipa locality. (H) Corroded graphite with dull and porous texture for a graphite grain from the Tanngarden locality.

4 | Analytical Techniques

Carbon and oxygen isotopic composition of dolomite/calcite and carbon isotope ratios of graphite were measured in this study. Calcite samples were separated using a knife-edge by scraping from a cut and polished slab of marble. The pulverised calcite was then placed in a small stainless steel cup and dropped into a reaction vessel containing concentrated phosphoric acid at 60°C for calcite and at 100°C for dolomite in a vacuum to liberate CO_2 (see Satish-Kumar, Kiran, and Abe 2021 for detailed analytical procedure). The liberated CO_2 gas was then purified cryogenically for analysis.

Graphite crystals, from the same hand specimens in which dolomite/calcite was analysed, were hand-picked from the residue of rock chips after the dissolution of carbonate with 6 N HCl. The graphite crystals were introduced into quartz glass tubes and an appropriate amount of vanadium pentoxide was added as an oxidising agent. The quartz glass tubes were preheated at 1100°C for 10 h, before sample introduction, to remove any contamination from the tubes (Wada, Fujii, and Niitsuma 1984). The graphite samples with vanadium pentoxide were again preheated at 500°C for 30 min to remove any surficial contamination in the sample/reagent. The tubes were then sealed in a vacuum and then allowed to combust for 2 h at 1000°C. The evolved CO_2 is completely used for measuring the isotopes.

The carbonate C–O isotope measurements were carried out with a Finnigan MAT-251 mass spectrometer (see Otsuji et al. 2013 for detailed analytical procedure) and carbon isotopes of graphite using Thermo-Fischer MAT-253 mass spectrometer (see Satish-Kumar, Kiran, and Abe (2021) for detailed analytical procedure), both instruments are housed at Niigata University. Machine standards calibrated to NBS-20 standard yield a $\delta^{13}C$ reproducibility of 0.05‰ for graphite and 0.03‰ for carbonate, and $\delta^{18}O$ of 0.05‰ (Satish-Kumar, Kiran, and Abe 2021) The

results are reported in conventional δ notation related to the V-PDB standard for carbon and V-SMOW standard for oxygen. The results of isotopic compositions are given in Table 3.

5 | Results

5.1 | Carbon and Oxygen Isotopic Composition of Dolomite/Calcite

Carbon and oxygen isotopic results of dolomite/calcite and carbon isotope ratios of graphite are presented in Table 3. Multiple analyses from single-hand specimens as well as analyses of multiple samples from selected localities were performed to confirm the homogeneity of their isotopic compositions. The metacarbonate rocks from the SRM show a broad range of values (Figure 7). The $\delta^{13}C_{VPDB}$ and $\delta^{18}O_{VSMOW}$ values of 24 metacarbonate samples range between −5.5‰ to +3.7‰ and +13.1‰ to +25.8‰, respectively (Table 3; Figure 7). The majority of samples, with the exception of two, one from Balchenfjella and one from Tanngarden, have $\delta^{18}O_{VSMOW}$ values in a narrow range between 20‰ and 25‰, which are comparable to the range of values shown by the Proterozoic carbonates (Eichman and Schidlowski 1975; Valley 1986; Knauth and Kennedy 2009; Satish-Kumar et al. 2021), thus indicating the preservation of pre-metamorphic isotope compositions. The $\delta^{13}C_{VPDB}$ values of dolomite/calcite are relatively homogeneous within a single coarse grain as well as in hand specimen (Figure 7), however, show variations between samples in a thick layer. Dolomite in contact with graphite does not show any variation in $\delta^{13}C_{VPDB}$ values. The variations observed in the $\delta^{13}C_{VPDB}$ values are larger than usually observed in high-grade metacarbonate rocks (cf. Satish-Kumar et al. 2021).

Outcrop-scale variations were tested across a thick layer at Balchenfjella (samples Balhen 5A-F; Table 3) extending for about 30 m, where six samples were collected at different intervals across the strike. The $\delta^{13}C_{VPDB}$ and $\delta^{18}O_{VSMOW}$ values range between −3.7‰ to −1.6‰ and +22.3‰ to +24.9‰, respectively (Figure 7), suggesting only minor variations within this layer. The largest $\delta^{13}C_{VPDB}$ variation is observed in sample Balchen-6F where the values vary between −3.9‰ to −5.5‰, intriguingly the oxygen isotope values do not vary much (+20.6‰ ±0.3‰; $n = 5$).

5.2 | Carbon Isotopic Composition of Graphite

The carbon isotope systematics in metacarbonate rocks are controlled by several factors. The isotopic systematics of organic carbon and carbonate carbon and their carbon isotopic composition have not varied much through time in the history of Earth (Strauss and Moore 1992). During metamorphism the carbon isotopic composition of organic materials changes by devolatilisation and exchange with carbonate carbon. The $\delta^{13}C_{VPDB}$ values of carbonate carbon are lowered to some extent, in the order of a few ‰, whereas the $\delta^{13}C_{VPDB}$ values of graphite will be increased in the order of 10‰ depending on the temperature of metamorphism. Other factors that control the isotopic distribution of carbonate carbon and graphitic carbon is the presence, inflow or

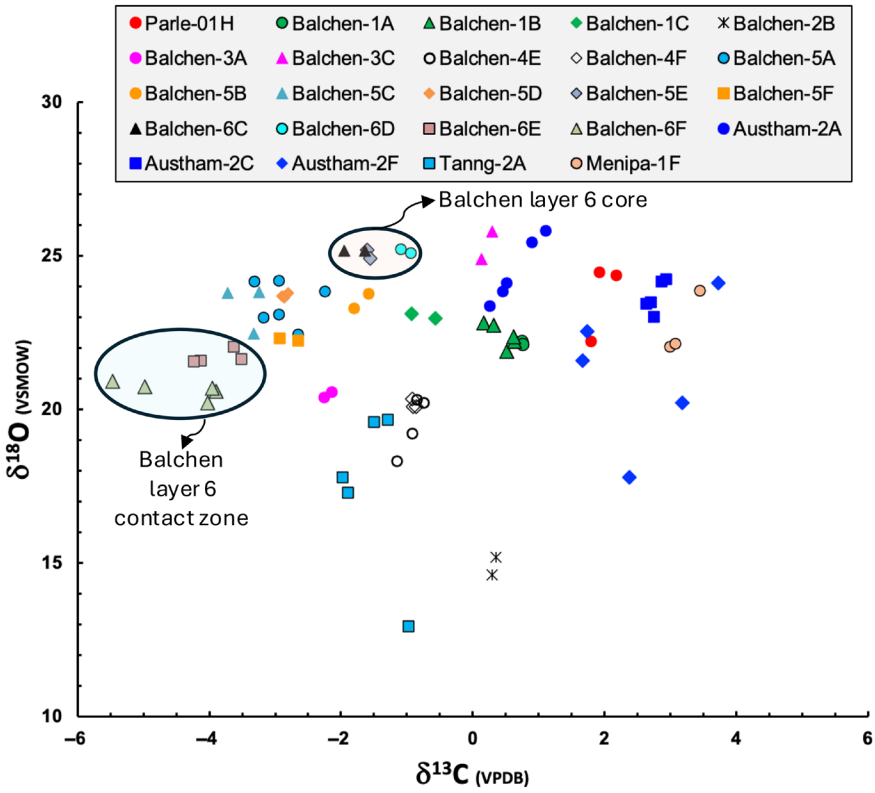

FIGURE 7 | Carbon and oxygen isotopic composition of metacarbonate rocks from the Sør Rondane Mountains. Note the carbon isotope values of the core part of the layer are showing higher $\delta^{13}C_{VPDB}$ and $\delta^{18}O_{VSMOW}$ values than the samples in the contact zone indicating the effect of fluid infiltration during retrogression.

outflow of CO_2 in the system such as progressive decarbonation reactions which release CO_2 (Harely and Santosh 1995) or external influx of carbon-bearing fluids to metacarbonate rocks (see Satish-Kumar, Wada, and Santosh 2002; Satish-Kumar et al. 2011). The metacarbonate rocks in the present study have modal carbonate contents of > 90% with appreciable amounts of crystalline graphite. Calc-silicate minerals are present only in minor amounts and hence, the carbon isotope systematics can be restricted to the calcite + graphite ± fluid system, and the effect of decarbonation has only a limited effect.

Table 3 shows the results of carbon isotope analyses of multiple grains of graphite in all 24 metacarbonate rock samples from six localities in the SRM. A total of 85 graphite crystals were analysed. In contrast to the generally homogenous carbon isotopic composition of dolomite/calcite, the $\delta^{13}C_{VPDB}$ values of graphite in some samples exhibited large variations as explained below.

The carbon isotopic composition of single graphite crystals shows variation in $\delta^{13}C_{VPDB}$ values. Multiple graphite crystals were analysed, and the results show variations between samples from −13.5‰ to +1.2‰ (Figure 8). However, the majority of the samples (22 out of 24) shows homogeneous carbon isotopic composition within the specimen, with deviations less than 1‰ from the average values. Two sample, both from Balchenfjella area (Balchen-5A and Balchen-6E) collected from the eastern contact of the layer with metapelitic rocks exhibited large-scale carbon isotopic heterogeneity. Six single crystals of graphite analyses for the Balchen-5A sample displayed variations in $\delta^{13}C_{VPDB}$ values that range from −12.0‰ to −6.5‰, whereas six individual graphite grains from sample Balchen-6E displayed a range of values between −13.5‰ and −4.3‰ (Table 3; Figure 8). Visual estimates of graphite grain size during sample preparation, indicate no systematic relationship between its size and carbon isotopic compositions (Table 2).

5.3 | In Situ Sampling of Carbonate Grains and Dolomite-Graphite Pairs

In situ sampling of carbonate for C–O isotopes was carried out in polished slabs (Figure 9A,B). Care was taken to avoid recrystallised grains or fine grain size, which potentially result in isotopic re-equilibration. For example, all five analyses of the core of dolomite in sample Austham 2C-1 showed similar values for carbon, whereas $\delta^{18}O$ values show only a slight difference of 1.2 (Figure 9A). In contrast, the fine-grained recrystallised grain boundaries in sample Austham 2F-1 have large differences in both carbon and oxygen isotopes (Figure 9B). The core of large grains gave the highest values of 3.7‰ and 24.2‰ for $\delta^{13}C_{VPDB}$ and $\delta^{18}O_{VSMOW}$ values, respectively. However, the grain boundary and recrystallised fine-grained dolomite gave values of 1.7‰ and 21.6‰ for $\delta^{13}C_{VPDB}$ and $\delta^{18}O_{VSMOW}$, respectively, suggesting a clear isotopic depletion for both carbon and oxygen in grain boundaries.

Separate slabs from the two samples described above were selected for further investigations on in situ dolomite-graphite

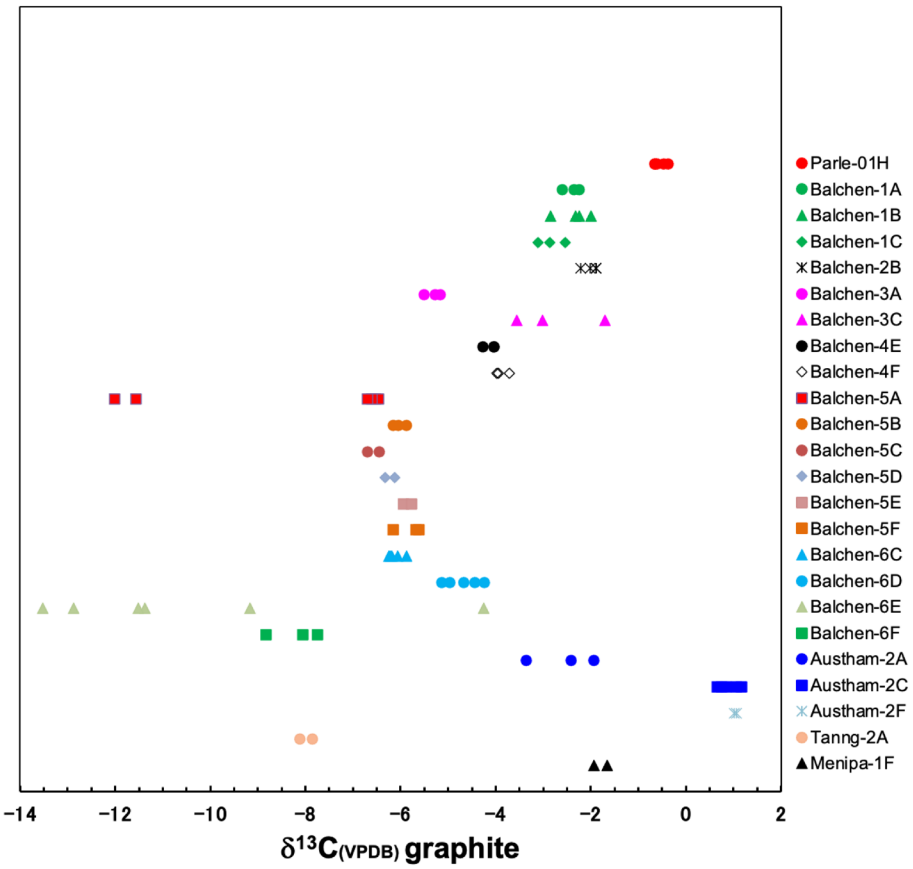

FIGURE 8 | Carbon isotopic composition of multiple graphite grains in metacarbonate rocks from the Sør Rondane Mountains. Note the large spread of values in two specific samples (Balchen 5A and 6E).

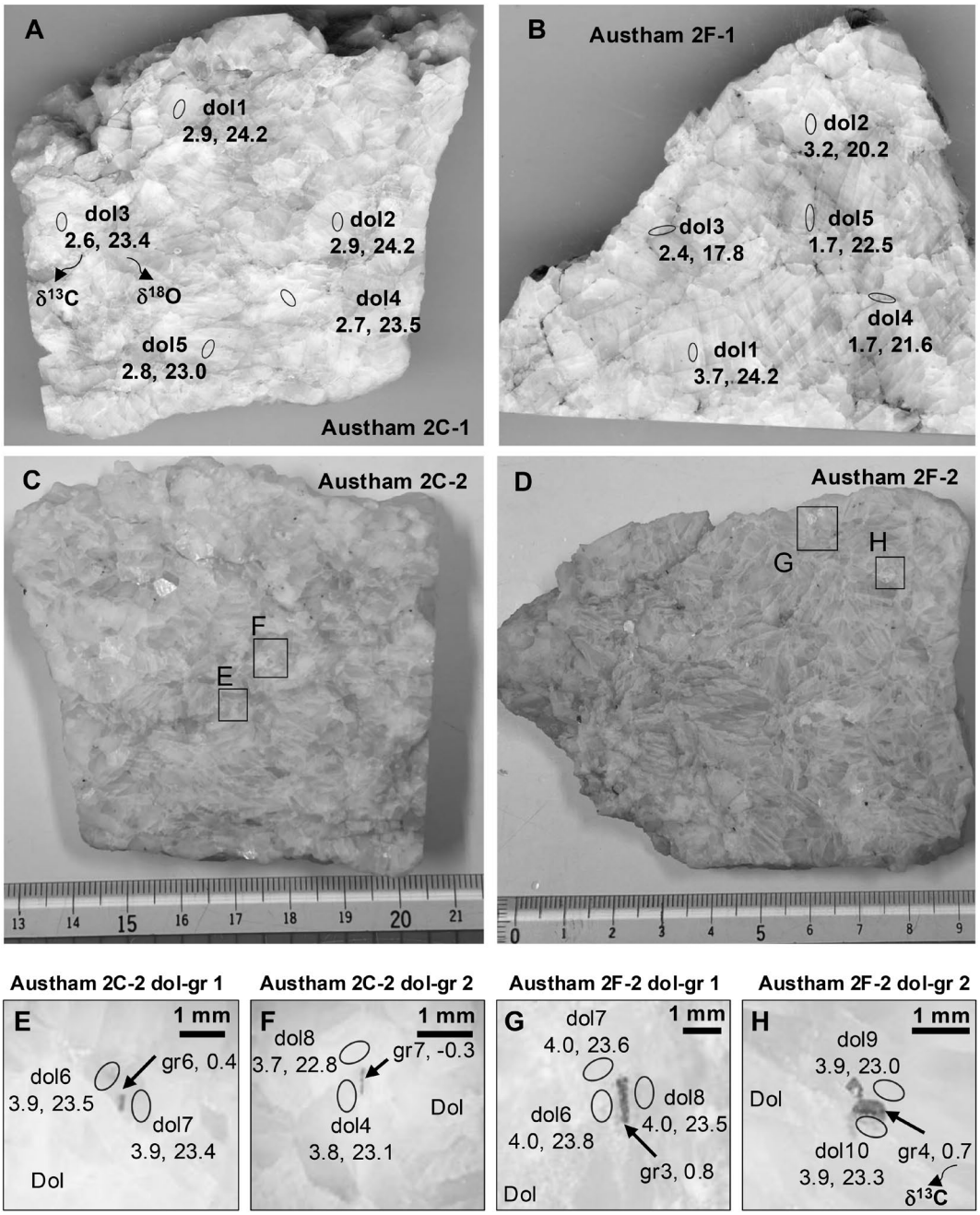

FIGURE 9 | Carbon and oxygen isotopic composition of dolomite in two slabs, one showing homogeneous values (A) and the other showing large heterogeneity (B). These two samples were further investigated for in situ carbon isotope analyses of dolomite-graphite pairs as shown in (C) and (D). E–H show the domains with graphite and dolomite which were analysed. See text for further details.

pair analysis as shown in Figure 9E–H. The results indicate that the grain boundary in contact with graphite is showing $\delta^{13}C_{VPDB}$ and $\delta^{18}O_{VSMOW}$ values which are similar to the core in Austham 2C-2 (Figure 9E,F), whereas the sample Austham 2F-2 has variations in both carbon and oxygen isotopic compositions (Figure 9G,H). These results will be discussed in detail from a carbonic fluid infiltration perspective.

5.4 | Carbon Isotope Thermometry

During prograde metamorphism carbon isotopes fractionate between the carbonate carbon and organic carbon with increasing temperature (Bottinga 1969). This isotopic fractionation was calibrated as a geothermometer and several studies have verified its application to varying metamorphic conditions (e.g., Valley and O'Neil 1981; Dunn and Valley 1992; Wada and Suzuki 1983; Kitchen and Valley 1995; Satish-Kumar and Wada 2000; Satish-Kumar, Wada, and Santosh 2002; Dunn 2005; Mizuochi et al. 2010; Dunn et al. 2019; Kim, Kim, and Lim 2020; Kiran et al. 2022). The fractionation of carbon isotopes between the carbonate and graphite decrease with temperature which is expressed as $\Delta^{13}C_{Cc\text{-}Gr}$. Several theoretical, empirical and experimental calibrations based on $\Delta^{13}C_{Cc\text{-}Gr}$ versus temperature have been proposed (Chacko et al. 1991; Scheele and Hoefs 1992; Dunn and Valley 1992; Kitchen and Valley 1995) and discussed

their validity under varying metamorphic conditions. For example, Kitchen and Valley (1995) have discussed in detail on the discrepancies between the calibrations, and they deduced a best-suited empirical calibration for granulite facies marbles. The empirical calibration of Dunn and Valley (1992) is suitable for lower-temperature amphibolite facies marbles and other studies indicate that several petrological thermometry results agree with the calibration of Wada and Suzuki (1983). Moreover, metamorphic temperature from amphibolite to greenschist facies can be deduced by careful sample selection before separation of graphite from the marbles (Wada and Suzuki 1983) and textural relationship between co-existing graphite in marble (Dunn and Valley 1992). The limitation of the application of the thermometry arises due to disturbances in equilibrium condition mainly due to the infiltration of external fluids and devolatilisation reactions (Kitchen and Valley 1995; Satish-Kumar, Wada, and Santosh 2002; Satish-Kumar et al. 2011). For this study, we estimated the temperature following the calibration of Kitchen and Valley (1995), since they were estimated using empirical or experimental results of higher temperature conditions (cf. Satish-Kumar, Wada, and Santosh 2002). In addition, previous studies of the SRM have shown that the region is metamorphosed under high temperature to UHT conditions (e.g., Hokada, Satish-Kumar, and Kawakami 2024 and references therein). The theoretical calibration of Polyakov and Kharlashina (1995) considered the effect of pressure on isotopic fractionation. Although the effect is less in medium to lower metamorphic grade, because of the large fractionation values, the effect is considerably enhanced due to small fractionation values at high to UHT conditions. For comparison, we have also provided the temperature estimates using Polyakov and Kharlashina (1995) calibration at 1 GPa. The calibrations of Dunn and Valley (1992) and Wada and Suzuki (1983) deviate much from Kitchen and Valley (1995) calibration at lower temperature conditions.

Carbon isotope fractionation between calcite and graphite (single crystals) is plotted in Figure 10. Considering the absence of isotopic heterogeneities in dolomite/calcite, average $\delta^{13}C_{VPDB}$ values were used in estimating the temperatures. Theoretical calibration of Polyakov and Kharlashina (1995) gave approximately 60°C lower temperature estimates for the range of metamorphic conditions in the samples examined, when compared with Kitchen and Valley (1995) calibration. The Kitchen and Valley (1995) calibration was chosen for estimating the temperatures because several previous studies have validated it for high-temperature conditions up to 850°C and they have excluded zoned graphite in calibrating the thermometer (e.g., Satish-Kumar, Wada, and Santosh 2002).

The temperatures estimated using carbon isotope thermometry for 24 metacarbonate samples from the SRM are shown in Figure 11. The peak metamorphic temperature from eight samples from Balchenfjella in the NE terrane is 802°C ± 29°C. UHT metamorphic conditions of 1032°C and 955°C were obtained from two samples from Balchenfjella (Balchen 1C and 2B). Seven samples displayed lower temperature conditions with larger variations in temperatures from 463°C to 746°C with an average of 647°C ± 93°C (Figure 10). Three samples from Austhamaren showed large variations in temperature estimates from 778°C to 900°C. The highest temperature estimate was provided by a sample which is in close proximity of the meta-igneous complex.

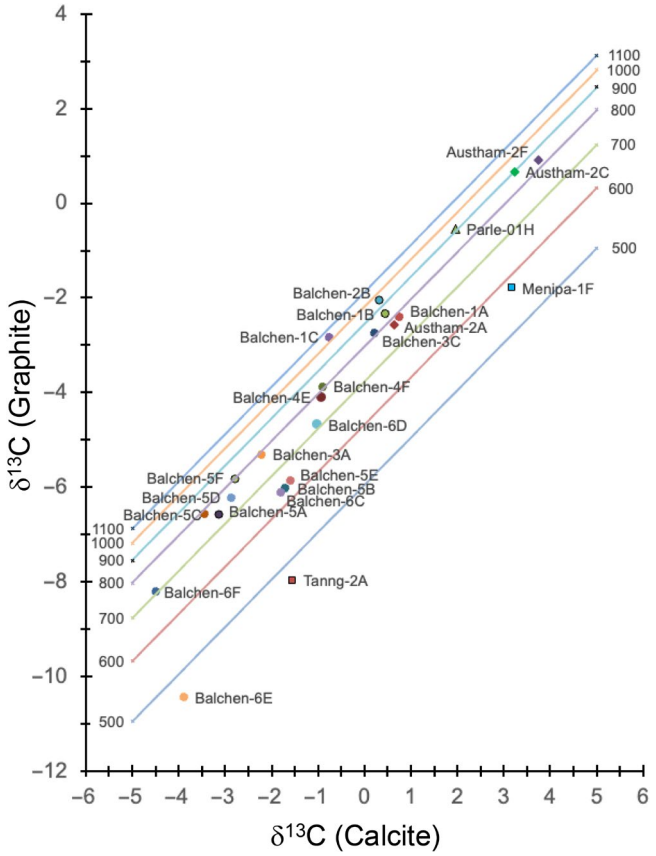

FIGURE 10 | Carbon isotopic composition of co-existing dolomite and graphite in metacarbonate rocks from the Sør Rondane Mountains. Isothermal lines are based on calcite-graphite thermometry calibration of Kitchen and Valley (1995).

The Perlebandet locality recorded high-temperature peak metamorphic conditions of 915°C. The Tanngarden locality recorded the lowest metamorphic temperature estimate of 470°C, whereas the sample from Menipa gave a temperature estimate of 603°C.

6 | Discussion

6.1 | Peak Metamorphic Temperature Conditions at the SRM

The relationship between the carbon isotopic composition of dolomite/calcite versus graphite indicates that the majority of the samples in the present study have variations in $\delta^{13}C_{VPDB}$ values; however, the fractionations fall in a short range (Figure 10), except for two samples. This is indicative of isotopic equilibrium between carbonate carbon and graphitic carbon, despite the variations in precursor compositions. These fractionation values reflect temperature conditions under which isotopic equilibrium has achieved as shown in Figure 11. Nine samples from Bachenfjella gave an average temperature condition of 802°C ± 29°C, suggesting peak temperature conditions during metamorphism. This estimate is comparable with the regional metamorphic conditions reported by Higashino et al. (2013a) and Grantham et al. (2013). However, two samples from the Balchenfjella locality (Balchen-1C and 2B) have lower carbon isotope fractionation

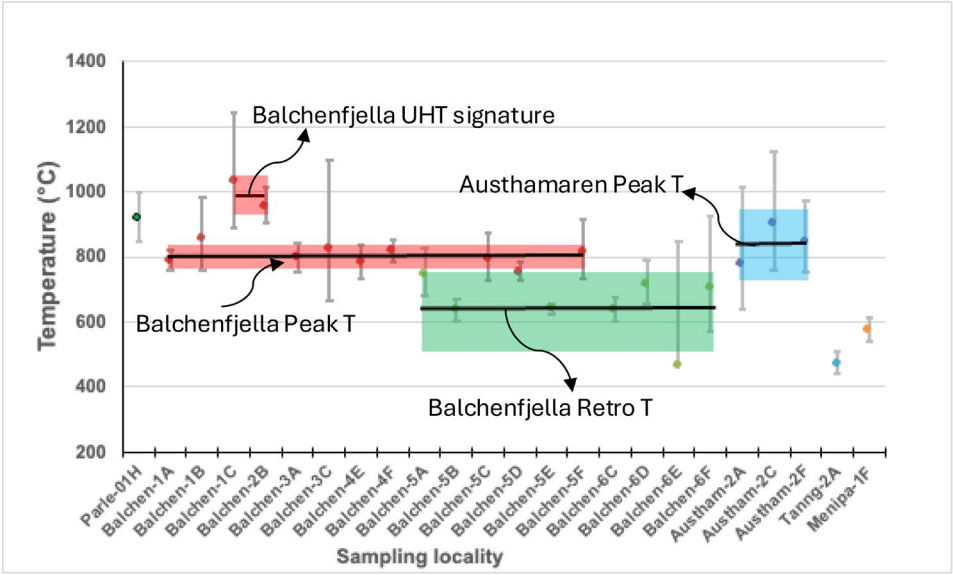

FIGURE 11 | Metamorphic temperature conditions recorded in metacarbonate rocks estimated using carbon isotope thermometry. The error bars represent the temperature estimated using the lowest and highest fractionation between carbonate and graphite. The solid line is the average for each locality with boxes showing the standard deviation (1σ). Note two specific samples, Balchen-1C and Balchen 2B, show high-temperature estimates in the UHT regime.

values, providing higher temperature estimates of 1032°C and 955°C. These results indicate that this locality might have experienced UHT conditions, which is consistent with the result of Higashino and Kawakami (2022). The textural and isotopic equilibrium between dolomite and graphite for Balchenfjella metacarbonate rocks provided accurate peak metamorphic temperature conditions for the region.

In this study, we have observed large variations in carbon isotope fractionation between dolomite and graphite at Austhamaren. To confirm the variations with respect to the textural locale of the sampling points, in situ isotope measurements were carried out (Figure 9). The results indicated that in samples with coarse equigranular dolomite display homogeneity in both $\delta^{13}C_{VPDB}$ and $\delta^{18}O_{VSMOW}$ values (Figure 9A), whereas those having grain boundary recrystallisation of the large dolomite crystals, there is a lowering of both $\delta^{13}C_{VPDB}$ and $\delta^{18}O_{VSMOW}$ values (Figure 9B). Further investigation of contact pairs of dolomite and graphite, gave homogeneous isotopic values (Figure 6E–H) and equilibrium carbon isotope fractionation (Figure 10). These fractionation values are consistent with the regional high-temperature metamorphic conditions reported for the region (Figure 11).

Carbon isotopic variations are prominent in samples, which were collected close to the meta-igneous intrusion, which might have resulted in a thermal impact as well as ingress of fluids to the surrounding lithologies. Dunn and Valley (1992) have examined the calcite-graphite carbon isotope system for marbles at Tudor Gabbro contact aureoule in the Greenville Province of Ontario, Canada, where they found that the carbon isotope system in marble is efficient enough to preserve the contact metamorphic temperature conditions within the aureoule whereas those away from the aureoule record only regional peak metamorphism. Austhamaren metacarbonate rocks possibly record a similar situation, where the samples in the vicinity of the meta-igneous rocks record higher temperature conditions, whereas those away record peak conditions equivalent to the regional metamorphic conditions (Figure 11).

At the Palebandet locality, we have obtained a peak temperature condition of 915 + 81/−66°C for a metacarbonate rock. The temperature conditions are consistent with the previous reports based on ternary feldspar thermometry in metapelitic rocks (Higashino et al. 2023b) and Zr-in-rutile thermometry (Kawakami et al. 2017). They reported a broad range of temperature conditions of 770°C–900°C, which is mostly consistent with the carbon isotope thermometry results in this study. Thus, the application of carbon isotope thermometry helped to extract the peak metamorphic temperature conditions in several localities where accurate metamorphic temperature conditions are not previously reported in detail.

6.2 | Retrograde Metamorphic Conditions

A detailed evaluation of 15 closely spaced and systematically collected samples from 5 metacarbonate layers in the Balchenfjella locality leads us to the identification of two retrograde events in the region. The first event is supposed to have occurred at temperature conditions around 650°C as can be seen from the consistent increase in the carbon isotope fractionation between dolomite and graphite in several samples (e.g., Balchen-5B, 5E and 6C). These samples were collected from the interior of the metacarbonate layers. Layer 5 metacarbonate unit is characterised by the presence of numerous secondary veins. Otsuji et al. (2013) suggested that the fluid infiltration causing these veins to have perturbated the trace element characteristics and the Sr. isotopic composition, although carbon and oxygen isotopic composition of carbonate could not be differentiated from the other samples unaffected by the event. Higashino et al. (2013a) has succeeded in delineating a near-peak Cl-rich fluid infiltration at ~800°C and a post-peak Cl-poor fluid infiltration at

> 540°C from the Balchenfjella locality, which is consistent with our estimates of retrograde resetting of the dolomite-graphite carbon isotope system.

The second event of fluid–rock interaction is clearly recorded in the samples collected in the eastern contact of the metacarbonate rocks with pelitic rocks. Samples Balchen-5A and Balchen-6E were both collected from within a meter from the contact zone and both samples exhibited large carbon isotope heterogeneity in graphite and a general lowering of carbon isotopic composition in both graphite and dolomite compared to the samples collected from the central portions of the layer (Table 3). The isotopic composition of graphite and dolomite shows a shift towards negative values indication a ^{12}C enriched fluids have disturbed the system. The textural observations in graphite also indicated overgrowth of smaller grains on pre-existing coarser flakes (Figure 6). Although it is difficult to specify which isotope values are in equilibrium with carbonate in these samples, the highest fractionation values may reflect temperature conditions lower than 500°C for this event. CO_2 fluid infiltration can disturb the carbonate-graphite equilibrium in metacarbonate rocks as described in some previous case studies. From a locality in the Southern Granulite Terrane in Peninsular India, Satish-Kumar, Wada, and Santosh (2002) described a marble outcrop where both carbon and oxygen isotopes in carbonates and carbon isotopic composition in graphite were lowered, along with an increase in graphite content. The isotopic disequilibrium in such a case was interpreted to be resulting from a carbonic fluid infiltration. In yet another study on calcite-graphite disequilibrium in the marble samples from Naxos, Satish-Kumar et al. (2011) reported fine-grained skeletal overgrowth textures in graphite grains, which was again interpreted to have resulted from graphite growth during carbonic fluid infiltration event. The overgrowth of small polygonal grains on pre-existing large flakes (Figure 6B,C) suggest fluid enhanced growth of graphite. In addition, both carbon and oxygen isotopic composition of dolomite shows lowering of values nearer to the contact zones suggesting that the carbonic fluids might have moved into the system along lithological contacts.

At Menipa locality a temperature condition of 572°C ± 30°C was estimated. This estimate is approximately 200°C lower than the existing inferences on metamorphic grade based on *P–T–t* path analysis using thermobarometries and mineral assemblages (Kawakami et al. 2022). Textural observations of graphite crystals show rough and overgrowth structures in the graphite crystal with skeletal overgrowth (Figure 6G). These features are indicative of late stage graphite growth possibly associated with fluid infiltration events, which need to be evaluated in further detailed studies.

At Tanngarden, which is located in the SW terrane with lower amphibolite facies conditions previously reported, the carbon isotope thermometry results indicated lower temperature conditions of 470 + 37/−32°C. Textural observation of graphite crystals indicates a corroded and porous texture, which is completely different from graphite grains that display carbon isotope equilibrium fractionation with carbonate. Field and petrographic evidence indicate extensive epidote formation during retrogression (Figure 3H), suggesting infiltration of hydrous fluids. This fluid infiltration event might have resulted in partial oxidation of pre-existing graphite forming a corroded texture and isotopic re-equilibration of the carbonate, that resulted in the lower temperature estimates (Figure 11).

6.3 | Reasons for Carbon Isotopic Disequilibrium

There are previous reports on carbon isotopic disequilibrium in calcite-graphite system even at high temperatures (e.g., Kreulen and Van Beek 1983; Arneth et al. 1985; Satish-Kumar, Wada, and Santosh 2002; Satish-Kumar et al. 2011). Textural characteristics of graphite are often used as a sensitive indicator of carbon isotopic equilibrium between carbonate and graphite. Studies have shown that highly crystalline graphite in marbles normally preserve isotopic signatures of peak metamorphic equilibration (Arita and Wada 1990; Dunn and Valley 1992; Morrison and Barth 1993), whereas isotopic disequilibrium has been reported in lower grade marbles which comprises of less crystalline graphite (Kreulen and van Beek 1983; Satish-Kumar et al. 2011). The presence of highly crystalline hexagonal to semi-hexagonal shaped graphite flakes with smooth high reflecting surface is indicative of high-temperature origin with isotopic equilibrium. Arita and Wada (1990) have pointed out that dull surfaced graphite results from the overgrowth of graphite on earlier coarse flakes, which are not common in samples of this study. Detailed textural analysis was carried out to exclude graphite samples that show rough surfaces or those with fine-grained overgrowth texture to overcome this limitation in carbon isotope thermometry. Furthermore, Kitchen and Valley (1995) and Satish-Kumar, Wada, and Santosh (2002) employed exfoliation of single graphite crystals to explore the carbon isotopic zonation, avoiding samples affected by retrograde isotope disequilibrium.

The carbon isotopic composition of graphite grains in two samples from Balchenfjella displays large variations between −4.3‰ and −13.5‰ (Table 2; Figure 6). Both these samples were collected from the eastern contact of metacarbonate with metapelitic rocks (Figure 3D). A close evaluation of the isotopic composition of dolomite in the whole layer suggest that the samples collected from the central domains of the layer display the highest $\delta^{13}C_{VPDB}$ and $\delta^{18}O_{VSMOW}$ values of −0.9‰ and +25.2‰, respectively, whereas the samples collected from the contact zone with pelitic rocks display lower values of −5.5‰ and +20.9‰. The carbon isotopic composition of graphite also displays a large variation from −4.2‰ in the central domain, whereas the contact zone towards the east display values as low as −13.5‰. Graphite precipitation from carbonic fluid haa been proposed in several previous studies (e.g., Harley and Santosh 1995; Farquhar, Hauri, and Wang 1999; Santosh et al. 2003) A recent study on the graphite formation at contact zones between pelitic and carbonate rocks at Lützow–Holm Complex suggested that fluid pooling at contact zones can result in concentration of graphite (Satish-Kumar 2023). Fluid infiltration events can also lead to isotopic disequilibrium between graphite and carbonates (Satish-Kumar, Wada, and Santosh 2002; Satish-Kumar et al. 2011; Kiran et al. 2022). Although in the case of Balchenfjella, the source of fluids has not been clarified yet, fluids might have emanated from the devolatilisation of organic materials in pelitic rocks. Wada et al. (1994) suggested that the fluids generated during devolatilisation of organic matter will

be highly depleted in ^{13}C. When such carbon-bearing fluids infiltrate into rocks under reducing conditions would precipitate/recrystallise new graphite (Lamb and Valley 1984). Farquhar, Hauri, and Wang (1999) suggest that the heterogeneous carbon isotopic zonation in graphite can result if a fluid varies in composition due to graphite precipitation.

Infiltration of low $\delta^{13}C_{VPDB}$-bearing fluids such as CO_2 can be a possible candidate for the observed isotopic disequilibrium between carbonate and graphite. Balchenfjella region is well known for retrograde fluid infiltration events, documented in several case studies (e.g., Higashino et al. 2013a, 2013b; Uno, Okamoto, and Tsuchiya 2017). These fluid infiltration events are clearly evident in metacarbonate rocks in the form of cross-cutting veins (Figure 3E,F) as well as formation of skarn along contact zones (Figure 3D,G). An episode of post-peak metamorphic fluid infiltration, while the granulites were still in the high temperature conditions can produce uniform $\delta^{13}C_{VPDB}$ values and $\delta^{18}O_{VSMOW}$ values in carbonate and with overgrowths in graphite. Kitchen and Valley (1995) and Satish-Kumar, Wada, and Santosh (2002) have shown that carbon isotope zonation in the order of several per mil within single graphite grains is indicative of isotopic exchange with fluids emanating either from decarbonation reactions or through the external influx of CO_2 fluids from the deeper crust. The Balchenfjella metacarbonate rocks in the contact zones with surrounding rocks as well as near the veins notably have lower $\delta^{13}C_{VPDB}$ and $\delta^{18}O_{VSMOW}$ values than the central domains of the layers suggesting that the fluid influx has caused this isotopic depletion in carbonate minerals.

6.4 | Robustness of Carbon Isotope Thermometry to Detect Multiple Thermal Events

Carbon isotope thermometry has proven to be an alternate way of clarifying peak metamorphic temperature conditions in many terranes. The robustness of this method lies in the sluggishness of carbon isotope exchange for graphite during retrograde metamorphism, since the diffusion rate of carbon in graphite is extremely slow (Thrower and Mayor 1978). Careful comparison of isotopic studies with Raman spectroscopy of carbonaceous materials has also proven the fact that carbon isotope thermometry can be applied for low-grade metamorphic conditions (e.g., Wada and Suzuki 1983; Kiran et al. 2022). Furthermore, previous studies have also suggested that carbon isotope thermometry can be used to detect polymetamorphism (e.g., Dunn and Valley 1992; Morrison and Barth 1993; Kitchen and Valley 1995; Bergfeld, Nabelek, and Labotka 1996). In the absence of a third carbon-bearing phase, the carbon isotope thermometry has provided reliable peak temperature conditions in high temperature and UHT metamorphism (e.g., Satish-Kumar, Wada, and Santosh 2002).

We report here for the first time, dolomite-graphite fractionations of less than 2‰ in metacarbonate rocks from the SRM regions in East Antarctica indicating clear evidence for UHT metamorphism. It is also significant that our data is in excellent agreement with the field evidence of contact metamorphic effects of a leuconorite intrusion, which occurs very nearthe metacarbonate outcrop. In addition, the carbon isotope thermometry also helped to detect multiple retrograde thermal events at the Balchenfjella locality. Whether these events are part of a single tectonothermal event or separate events needs to be further evaluated through detailed studies.

7 | Conclusions

The following conclusions were obtained in this study.

1. Carbon isotope thermometry of a suite of metacarbonate rocks provided peak and retrograde metamorphic temperature estimates for the Sør Rondane Mountains in East Antarctica.
2. Ultrahigh-temperature metamorphic signatures were observed in the couple of samples from the Balchenfjella locality.
3. Variations in carbon isotope fractionation values in Austhamaren locality could be an effect of contact metamorphism.
4. Consistent peak temperature estimates of 800°C–850°C are reported for the Balchenfjella locality.
5. Retrograde metamorphic conditions re-equilibrated the carbonate-graphite carbon isotope system to some extent and temperature conditions could be constrained.
6. Disequilibrium graphite crystal growth from external carbon-bearing fluids might be the reason for the deviations in fractionation between carbonate and graphite at contact zones of metacarbonate rocks with metapelitic rock units.

The above conclusions suggest the robustness of carbon isotope thermometry in deducing the metamorphic evolution of terranes affected by multiple metamorphic and fluid infiltration events.

Author Contributions

M. Satish-Kumar: field work and sample collection, conceptualization, data acquisition and interpretation, manuscript draft preparation, reviewing and editing. **Sasidharan Kiran:** data acquisition and interpretation, manuscript reviewing and editing. **Tetsuo Kawakami:** field work and sample collection, data interpretation, manuscript reviewing and editing. **Fumiko Higashino and Tetsuo Hokada:** data interpretation, manuscript reviewing and editing.

Acknowledgements

We thank Prof. Tsuchiya and all JARE-51 members in the Sør Rondane Expedition for their help during the field survey. Ms. Naho Otsuji helped in measuring carbonate C–O analysis using MAT-251 mass spectrometer. This work was supported by the Grants-in-Aid for Scientific Research (KAKENHI) of the Japan Society for the Promotion of Science (JSPS) Nos. JP15H05831, JP20KK0081, JP22H04932, JP21H01182. We thank the reviewer for constructive criticism that helped to modify the manuscript and clarify the relation between observed isotopic heterogeneity and temperature estimates.

Data Availability Statement

All data included in the manuscript.

Peer Review

The peer review history for this article is available at https://www.webofscience.com/api/gateway/wos/peer-review/10.1002/gj.5095.

References

Adachi, T., T. Hokada, Y. Osanai, N. Nakano, S. Baba, and T. Toyoshima. 2013b. "Contrasting Metamorphic Records and Their Implications for Tectonic Process in the Central Sør Rondane Mountains, Eastern Dronning Maud Land, East Antarctica." In *Antarctica and Supercontinent Evolution*, edited by S. L. Harley, L. C. W. Fitzsimons, and Y. Zhao, vol. 383, 113–133. London: Geological Society of London, Special Publication.

Adachi, T., T. Kawakami, F. Higashino, and M. Uno. 2023. "Metamorphic Rocks With Different Pressure–Temperature–Time Paths Bounded by a Ductile Shear Zone at Oyayubi Ridge, Brattnipene, Sør Rondane Mountains, East Antarctica." *Journal of Mineralogical and Petrological Sciences* 118: S014.

Adachi, T., Y. Osanai, T. Hokada, N. Nakano, S. Baba, and T. Toyoshima. 2013a. "Timing of Metamorphism in the Central Sør Rondane Mountains, Eastern Dronning Maud Land, East Antarctica: Constrains From SHRIMP Zircon Dating and EPMA Monazite Dating." *Precambrian Research* 234: 136–160.

Arita, Y., and H. Wada. 1990. "Stable Isotope Evidence for Migration of Metamorphic Fluids Along Grain Boundaries of Marbles." *Geochemical Journal* 24: 173–186.

Arneth, J. D., M. Schidlowski, B. Sarbas, U. Goerg, and G. C. Amstutz. 1985. "Graphite Content and Isotopic Fractionation Between Calcite-Graphite Pairs in Metasediments From the Mgama Hills, Southern Kenya." *Geochimica et Cosmochimica Acta* 49: 1553–1560.

Asami, M., E. S. Grew, and H. Makimoto. 1990. "A Staurolite-Bearing Corundum-Garnet Gneiss From the Eastern Sør Rondane Mountains, Antarctica." *Proceedings of NIPR Symposium on Antarctic Geosciences* 4: 22–40.

Asami, M., E. S. Grew, and H. Makimoto. 2007. "Relict Sapphirine+Kyanite and Spinel+Kyanite Associations in Pyrope Garnet From the Eastern Sør Rondane Mountains, East Antarctica." *Lithos* 93: 107–125.

Asami, M., H. Makimoto, E. S. Grew, et al. 1991. "Geological Map of the Balchenfjella, Antarctica." In *Antarctic Geological Map Series, Sheet 31, Scale 1:50,000*. Tokyo: National Institute of Polar Research.

Asami, M., Y. Osanai, K. Shiraishi, and H. Makimoto. 1992. "Metamorphic Evolution of the Sør Rondane Mountains, East Antarctica." In *Recent Progress in Antarctic Earth Science*, edited by Y. Yoshida, K. Kaminuma, and K. Shiraishi, 7–15. Tokyo: Terra Scientific Publishing Company.

Bergfeld, D., P. I. Nabelek, and T. C. Labotka. 1996. "Carbon Isotope Exchange During Polymetamorphism in the Panamint Mountains, California, USA." *Journal of Metamorphic Geology* 14: 199–212.

Bottinga, Y. 1969. "Calculated Fractionation Factors for Carbon and Hydrogen Isotope Exchange in the System Calcite-Carbon Dioxide-Graphite-Methane-Hydrogen-Water Vapor." *Geochimica et Cosmochimica Acta* 33: 49–64.

Brown, M. 2006. "Duality of Thermal Regimes Is the Distinctive Characteristic of Plate Tectonics Since the Neoarchean." *Geology* 34: 961.

Brown, M. 2007. "Metamorphism, Plate Tectonics, and the Supercontinent Cycle." *Earth Science Frontiers* 14: 1–18.

Chacko, T., T. K. Mayeda, R. N. Clayton, and J. R. Goldsmith. 1991. "Oxygen and Carbon Isotope Fractionations Between CO_2 and Calcite." *Geochimica et Cosmochimica Acta* 55: 2867–2882.

Dienes, P., and D. H. Eggler. 2009. "Experimental Determination of Carbon Isotope Fractionation Between $CaCO_3$ and Graphite." *Geochimica et Comsmochimica Acta* 73: 7256–7274.

Dunn, S. R. 2005. "Calcite-Graphite Isotope Thermometry in Amphibolite Facies Marble, Bancroft, Ontario." *Journal of Metamorphic Geology* 23: 813–827.

Dunn, S. R., M. J. Markley, M. Kotikian, K. Achenbach, B. Montanye, and W. H. Peck. 2019. "Geothermometry of the Western Half of the Central Metasedimentary Belt, Grenville Province, Ontario, and Its Implications." *American Mineralogist* 104: 791–809.

Dunn, S. R., and J. W. Valley. 1992. "Calcite-Graphite Isotope Thermometry: A Test for Polymetamorphism in Marble, Tudor Gabbro Aureole, Ontario, Canada." *Journal of Metamorphic Geology* 10: 487–501.

Durgalakshmi, K. Sajeev, I. S. Williams, et al. 2021. "The Timing, Duration and Conditions of UHT Metamorphism in Remnants of the Former Eastern Gondwana." *Journal of Petrology* 62: 1–38.

Eichman, R., and M. Schidlowski. 1975. "Isotopic Fractionation Between Coexisting Organic Carbon-Carbonate Pairs in Pre-Cambrian Sediments." *Geochimica et Cosmochimica Acta* 39: 585–595.

Farquhar, J., E. Hauri, and J. Wang. 1999. "New Insights Into Carbon Fluid Chemistry and Graphite Precipitation: SIMS Analysis of Granulite Facies Graphite From Ponmudi, South India." *Earth and Planetary Science Letters* 171: 607–621.

Grantham, G. H., P. H. Macey, K. Horie, et al. 2013. "Comparison of the Metamorphic History of the Monapo Complex, Northern Mozambique and Balchenfjella and Austhamaren Areas Sør Rondane, Antarctica: Implications for the Kuunga Orogeny and the Amalgamation of N and S. Gondwana." *Precambrian Research* 234: 85–135.

Halverson, G. P., P. F. Hoffman, D. P. Schrag, A. C. Maloof, and A. H. Rice. 2005. "Towards a Neoproterozoic Composite Carbon-Isotope Record." *Geological Society of America Bulletin* 117: 1181–1207.

Harley, S. L. 1998. "On the Occurrence and Characterization of Ultrahigh-Temperature Metamorphism." In *What Drives Metamorphism and Metamorphic Reactions?* edited by P. J. Treloar and P. J. O'Brien, vol. 138, 81–107. London: Geological Society of London, Special Publication.

Harley, S. L. 2008. "Refining the P–T Records of UHT Crustal Metamorphism." *Journal of Metamorphic Geology* 26: 125–154.

Harley, S. L. 2021. "UHT Metamorphism." In *Encyclopedia of Geology*, edited by D. Alderton and S. A. Elias, 522–552. Amsterdam: Elsevier.

Harley, S. L., and M. Santosh. 1995. "Wollastonite at Nuliyam, Kerala, Southern India: A Reassessment of CO_2-Infiltration and Charnockite Formation at a Classic Locality." *Contributions to Mineralogy and Petrology* 120: 83–94.

Higashino, F., and T. Kawakami. 2022. "Ultrahigh-Temperature Metamorphism and Melt Inclusions From the Sør Rondane Mountains, East Antarctica." *Journal of Mineralogical and Petrological Sciences* 117: 010.

Higashino, F., T. Kawakami, T. Adachi, and M. Uno. 2023b. "Multiple Post-Peak Metamorphic Fluid Infiltrations in Southern Perlebandet, Sør Rondane Mountains, East Antarctica." *Journal of Mineralogical and Petrological Sciences* 118: S004.

Higashino, F., T. Kawakami, S. Sakata, and T. Hirata. 2023a. "Multiple Timings of Garnet-Forming High-Grade Metamorphism in the Neoproterozoic Continental Collision Zone Revealed by Petrochronology in the Sør Rondane Mountains, East Antarctica." *Gondwana Research* 119: 204–226.

Higashino, F., T. Kawakami, M. Satish-Kumar, et al. 2013a. "Chlorine-Rich Fluid or Melt Activity During Granulite Facies Metamorphism in the Late Proterozoic to Cambrian Continental Collision Zone—An Example From the Sør Rondane Mountains, East Antarctica." *Precambrian Research* 234: 229–246.

Higashino, F., T. Kawakami, M. Satish-Kumar, M. Ishikawa, N. Tsuchiya, and G. H. Grantham. 2013b. "Multi-Stage Cl-Rich Fluid Activity and Behavior of REE-Bearing Minerals in a Neoproterozoic Granulite Terrane. Goldschmidt 2013 Abstract." *Mineralogical Magazine* 77: 1298.

Higashino, F., T. Kawakami, N. Tsuchiya, et al. 2019a. "Brine Infiltration in the Middle to Lower Crust in a Collision Zone: Mass Transfer and Microtexture Development Through Wet Grain–Boundary Diffusion." *Journal of Petrology* 60: 329–358.

Higashino, F., D. Rubatto, T. Kawakami, A.-S. Bouvier, and L. P. Baumgartner. 2019b. "Oxygen Isotope Speedometry in Granulite Facies Garnet Recording Fluid/Melt–Rock Interaction (Sør Rondane Mountains, East Antarctica)." *Journal of Metamorphic Geology* 37: 1037–1048.

Hokada, T., T. Adachi, Y. Osanai, N. Nakano, S. Baba, and T. Toyoshima. 2022. "Formation of Corundum in Direct Contact With Quartz and Biotite in Clockwise P–T Trajectory From the Sør Rondane Mountains, East Antarctica." *Journal of Mineralogical and Petrological Sciences* 117: 220317.

Hokada, T., K. Horie, T. Adachi, et al. 2013. "Unraveling the Metamorphic History at the Crossing of Neoproterozoic Orogens, Sør Rondane Mountains, East Antarctica: Constraints From U–Th–Pb Geochronology, Petrography, and REE Geochemistry." *Precambrian Research* 234: 183–209.

Hokada, T., M. Satish-Kumar, and T. Kawakami. 2024. "Recent Advances in Mineralogy, Petrology, Geochemistry, and Geochronology in East Antarctica." *Journal of Mineralogical and Petrological Sciences* 119: S002.

Ishikawa, M., T. Kawakami, M. Satish-Kumar, et al. 2013. "Late Neoproterozoic Extensional Detachment in Eastern Sør Rondane Mountains, East Antarctica: Implications for the Collapse of East African Antarctic Orogen." *Precambrian Research* 234: 247–256.

Jöns, N., and V. Schenk. 2011. "The Ultrahigh Temperature Granulites of Southern Madagascar in a Polymetamorphic Context: Implications for the Amalgamation of the Gondwana Supercontinent." *European Journal of Mineralogy* 23: 127–156.

Kamei, A., K. Horie, M. Owada, et al. 2013. "Late Proterozoic Juvenile Arc Metatonalite and Adakitic Intrusions in the Sør Rondane Mountains, Eastern Dronning Maud Land, Antarctica." *Precambrian Research* 234: 47–62.

Kawakami, T., F. Higashino, T. Adachi, and M. Uno. 2021. "Decompression P–T Evolution Recorded in a Pelitic Gneiss From Tangarden, Sør Rondane Mountains, East Antarctica." In *Abstract of the Japan Geoscience Union Meeting 2021*. Tokyo: Japan Geoscience Union.

Kawakami, T., F. Higashino, E. Skrzypek, et al. 2017. "Pressure–Temperature–Time Path and Timing of Cl-Bearing Fluid Infiltration to the Upper-Amphibolite to Granulite Facies Metamorphic Rocks at Perlebandet, Sør Rondane Mountains, East Antarctica." *Lithos* 274–275: 73–92.

Kawakami, T., S. Niki, M. Suzuki, et al. 2022. "Pressure–Temperature–Time Path of Granulite Indicating Long-Lived Metamorphism in Collision Setting From Central Sør Rondane Mountains, East Antarctica." In *Abstract of the International Association of Gondwana Research Annual Meeting 2022*. Beijing: International Association for Gondwana Research.

Kelsey, D. E. 2008. "On Ultrahigh-Temperature Crustal Metamorphism." *Gondwana Research* 113: 1–29.

Kim, C., H. Kim, and C. Lim. 2020. "Carbon-Oxygen Isotope Records of Precambrian Metamorphic Rocks in the Yeongnam Massif Area, South Korea." *Precambrian Research* 346: 105739.

Kiran, S., M. Satish-Kumar, Y. Nakamura, and T. Hokada. 2022. "Comparison Between Raman Spectra of Carbonaceous Material and Carbon Isotope Thermometries in Low-Medium Grade meta-Carbonates: Implications for Estimation of Metamorphic Temperature Condition." *Precambrian Research* 374: 106656.

Kitano, I., Y. Osanai, N. Nakano, and T. Adachi. 2016. "Detrital Zircon Provenances for Metamorphic Rocks From Southern Sør Rondane Mountains, East Antarctica: A New Report of Archean to Mesoproterozoic Zircons." *Journal of Mineralogical and Petrological Sciences* 111: 118–128.

Kitchen, N., and J. W. Valley. 1995. "Carbon Isotope Thermometry in Marbles of the Adirondack Mountains, New York." *Journal of Metamorphic Geology* 13: 577–594.

Knauth, L. P., and M. J. Kennedy. 2009. "The Late Precambrian Greening of the Earth." *Nature* 460: 728–732.

Kreulen, R., and P. C. J. M. van Beek. 1983. "The Calcite-Graphite Isotope Thermometer; Data on Graphite-Bearing Marbles From Naxos, Greece." *Geochimica et Cosmochimica Acta* 47: 1527–1530.

Lamb, W. M., and J. W. Valley. 1984. "Metamorphism of Reduced Granulites in Low-CO_2 Vapour Free Environment." *Nature* 312: 56–58.

Mieth, M., J. Jacobs, A. Ruppel, D. Damaske, A. Läufer, and W. Jokat. 2014. "New Detailed Aeromagnetic and Geological Data of Eastern Dronning Maud Land: Implications for Refining the Tectonic and Structural Framework of Sør Rondane, East Antarctica." *Precambrian Research* 245: 174–185.

Mizuochi, H., M. Satish-Kumar, Y. Motoyoshi, and K. Michibayashi. 2010. "Exsolution of Dolomite and Application of Calcite-Dolomite Solvus Geothermometry in High-Grade Marbles: An Example From Skallevikshalsen, East Antarctic." *Journal of Metamorphic Geology* 28: 509–526.

Morikiyo, T. 1984. "Carbon Isotope Study of Co-Existing Calcite and Graphite in the Ryoke Metamorphic Rocks, Northern Kiso District, Central Japan." *Contributions to Mineralogy and Petrology* 87: 251–259.

Morrison, J., and A. P. Barth. 1993. "Empirical Tests of Carbon Isotope Thermometry in Granulites From Southern California." *Journal of Metamorphic Geology* 11: 789–800.

Nakano, N., Y. Osanai, A. Kamei, et al. 2013. "Multiple Thermal Events Recorded in Metamorphosed Carbonate and Associated Rocks From the Southern Austkampane Region in the Sør Rondane Mountains, East Antarctica: A Protracted Neoproterozoic History at the Gondwana Suture Zone." *Precambrian Research* 234: 161–182.

Osanai, Y., Y. Nogi, S. Baba, et al. 2013. "Geologic Evolution of the Sør Rondane Mountains, East Antarctica: Collision Tectonics Proposed Based on Metamorphic Processes and Magnetic Anomalies." *Precambrian Research* 234: 8–29.

Osanai, Y., K. Sajeev, N. Nakano, et al. 2016a. "UHT Granulites of the Highland Complex, Sri Lanka I: Geological and Petrological Background." *Journal of Mineralogical and Petrological Sciences* 111: 145–156.

Osanai, Y., K. Sajeev, N. Nakano, et al. 2016b. "UHT Granulites of the Highland Complex, Sri Lanka II: Geochronological Constraints and Implications for Gondwana Correlation." *Journal of Mineralogical and Petrological Sciences* 111: 157–169.

Osanai, Y., K. Shiraishi, Y. Takahashi, et al. 1992. "Geochemical Characteristics of Metamorphic Rocks From the Central Sør Rondane Mountains, East Antarctica." In *Recent Progress in Antarctic Earth Science*, edited by Y. Yoshida, K. Kaminuma, and K. Shiraishi, 17–27. Tokyo: Terra Scientific Publishing Company.

Osanai, Y., T. Ueno, N. Tsuchiya, Y. Takahashi, Y. Tainosho, and K. Shiraishi. 1990. "Finding of Vanadium-Bearing Garnet From the Sør Rondane Mountains, East Antarctica." *Antarctic Record* 34: 279–291.

Otsuji, N., M. Satish-Kumar, A. Kamei, et al. 2016. "Sr and Nd Isotopic Evidence in Metacarbonate Rocks for an Extinct Island Arc–Ocean System in East Antarctica." *Journal of Mineralogical and Petrological Sciences* 111: 170–180.

Otsuji, N., M. Satish-Kumar, A. Kamei, et al. 2013. "Late-Tonian to Early-Cryogenian Apparent Depositional Ages for Metacarbonate

Rocks From the Sør Rondane Mountains, East Antarctica." *Precambrian Research* 234: 257–278.

Owada, M., S. Baba, Y. Osanai, and H. Kagami. 2008. "Geochemistry of Post-Kinematic Mafic Dykes From Central to Eastern Dronning Maud Land, East Antarctica: Evidence for a Pan-African Suture in Dronning Maud Land." In *Geodynamic Evolution of East Antarctica: A Key to the East-West Gondwana Connection*, edited by M. Satish-Kumar, Y. Motoyoshi, Y. Osanai, Y. Hiroi, and K. Shiraishi, vol. 308, 235–252. London: Geological Society of London, Special Publications.

Owada, M., T. Shimura, M. Yuhara, A. Kamei, and K. Tsukada. 2010. "Post-Kinematic Lamprophyre From the Southwestern Part of Sør Rondane Mountains, East Antarctica: Constraint on the Pan-African Suture Event." *Journal of Mineralogical and Petrological Sciences* 105: 262–267.

Polyakov, V. B., and N. N. Kharlashina. 1995. "The Use of Heat Capacity Data to Calculate Carbon Isotope Fractionation Between Graphite, Diamond and Carbon Dioxide: A New Approach." *Geochimica et Cosmochimica Acta* 59: 2561–2572.

Ruppel, A. S., J. Jacobs, A. Läufer, et al. 2021. "Protracted Late Neoproterozic – Early Palaeozoic Deformation and Cooling History of Sør Rondane, East Antarctica, From 40Ar/39Ar and U–Pb Geochronology." *Geological Magazine* 158: 635–655.

Sajeev, K., and Y. Osanai. 2004. "Ultrahigh-Temperature Metamorphism (1150°C, 12 kbar) and Multistage Evolution of Mg-, Al-Rich Granulites From the Central Highland Complex, Sri Lanka." *Journal of Petrology* 45: 1821–1844.

Sajeev, K., Y. Osanai, and M. Santosh. 2004. "Ultrahigh-Temperature Metamorphism Followed by Two-Stage Decompression of Garnet-Orthopyroxene-Sillimanite Granulites From Ganguvarpatti, Madurai Block, Southern India." *Contributions to Mineralogy and Petrology* 148: 29–46.

Santosh, M., H. Wada, M. Satish-Kumar, and S. S. Binu-Lal. 2003. "Carbon Isotope 'Stratigraphy' in a Single Graphite Crystal: Implications for Crystal Growth Mechanism of Fluid Deposited Graphite." *American Mineralogist* 88: 1689–1696.

Satish-Kumar, M. 2000. "Ultrahigh-Temperature Metamorphism in Madurai Granulites, Southern India: Evidence From Carbon Isotope Thermometry." *Journal of Geology* 108: 479–486.

Satish-Kumar, M. 2023. "Carbon Isotopic Composition of Graphite in Metamorphic Rocks From Lützow–Holm Complex, East Antarctica: Implications for Carbon Geodynamic Cycle in Continental Crust." *Journal of Mineralogical and Petrological Sciences* 118: S017.

Satish-Kumar, M., T. Hokada, M. Owada, Y. Osanai, and K. Shiraishi. 2013. "Neoproterozoic Orgens Amalgamating East Gondwana: Did They Cross Each Other?" *Precambrian Research* 234: 1–7.

Satish-Kumar, M., J. A. Jaszczak, T. Hamamatsu, and H. Wada. 2011. "Relationship Between Structure, Morphology, and Carbon Isotopic Composition of Graphite in Marbles: Implications for Calcite-Graphite Carbon Isotope Thermometry." *American Mineralogist* 96: 470–485.

Satish-Kumar, M., S. Kiran, and M. Abe. 2021. "A New Inlet System for Microscale Carbon and Oxygen Stable Isotope Analysis Using Dual Isotope Ratio Mass Spectrometer at Niigata University, Japan." *Science Reports, Niigata University* 36: 21–42.

Satish-Kumar, M., M. Shirakawa, A. Imura, et al. 2021. "A Geochemical and Isotopic Perspective on Tectonic Setting and Depositional Environment of Precambrian meta-Carbonate Rocks in Collisional Orogenic Belts." *Gondwana Research* 96: 163–204.

Satish-Kumar, M., and H. Wada. 2000. "Carbon Isotopic Equilibrium Between Calcite and Graphite in Skallen Marbles, East Antarctica: Evidence for the Preservation of Peak Metamorphic Temperatures." *Chemical Geology* 166: 173–182.

Satish-Kumar, M., H. Wada, and M. Santosh. 2002. "Constraints on the Application of Carbon Isotope Thermometry in High- To Ultrahigh-Temperature Metamorphic Terranes." *Journal of Metamorphic Geology* 20: 335–350.

Scheele, N., and J. Hoefs. 1992. "Carbon Isotope Fractionation Between Calcite, Graphite and CO_2: An Experimental Study." *Contributions to Mineralogy and Petrology* 112: 35–45.

Sheppard, S. M. F., and H. P. Schwarz. 1970. "Fractionation of Carbon and Oxygen Isotopes and Magnesium Between Co-Existing Calcite and Dolomite." *Contributions to Mineralogy and Petrology* 26: 161–198.

Shiraishi, K., M. Asami, H. Ishizuka, et al. 1991. "Geology and Metamorphism of the Sør Rondane Mountains, East Antarctica." In *Geological Evolution of Antarctica*, edited by M. R. A. Thomson, J. A. Crame, and J. W. Thomson, 77–82. Cambridge: Cambridge University Press.

Shiraishi, K., D. J. Dunkley, T. Hokada, C. M. Fanning, H. Kagami, and T. Hamamoto. 2008. "Geochronological Constrains on the Late Proterozoic to Cambrian Crustal Evolution of Eastern Dronning Maud Land, East Antarctica: A Synthesis of SHRIMP U–Pb Age and Nd Model Age Data." In *Geodynamic Evolution of East Antarctica: A Key to the East-West Gondwana Connection*, edited by M. Satish-Kumar, Y. Motoyoshi, Y. Osanai, Y. Hiroi, and K. Shiraishi, vol. 308, 21–67. London: Geological Society of London, Special Publications.

Shiraishi, K., Y. Osanai, H. Ishizuka, and M. Asami. 1997. "Geological Map of the Sør Rondane Mountains, Antarctica." In *Geological Map Series, Sheet 35, Scale 1:250,000*. Tokyo: National Institute of Polar Research.

Strauss, H., and T. B. Moore. 1992. "Abundances and Isotopic Compositions of Carbon and Sulfur Species in Whole Rock and Kerogen Samples." In *The Proterozoic Biosphere, A Multidisciplinary Study*, edited by J. W. Schopf and C. Klein, 709–798. New York: Cambridge University Press.

Suzuki, K., and T. Kawakami. 2019. "Metamorphic Pressure–Temperature Conditions of the Lützow–Holm Complex of East Antarctica Deduced From Zr-in-Rutile Geothermometer and Al_2SiO_5 Minerals Enclosed in Garnet." *Journal of Mineralogical and Petrological Sciences* 114: 267–279.

Thrower, P. A., and R. M. Mayor. 1978. "Point Defects and Self Diffusion in Graphite." *Physica Status Solidi* 47: 11–37.

Tsubokawa, Y., M. Ishikawa, T. Kawakami, et al. 2017. "Pressure–Temperature–Time Path of a Metapelite From Mefjell, Sør Rondane Mountains, East Antarctica." *Journal of Mineralogical and Petrological Sciences* 112: 77–87.

Tsuchiya, N., M. Ishikawa, M. Satish-Kumar, et al. 2012. "Report on Geological Fieldwork in the Sør Rondane Mountains, Eastern Dronning Maud Land, 2009–2010 (JARE-51)." *Antarctic Record* 56: 295–379.

Tsukada, K., P. Sukhbaatar, M. Owada, et al. 2023. "Tectonic Division of the Southwestern Terrane at the Western Sør Rondane Mountains, Dronning Maud Land, East Antarctica, From a Viewpoint of Zircon U–Pb Ages." *Journal of Mineralogical and Petrological Sciences* 118: S013.

Tsunogae, T., and M. Santosh. 2006. "Spinel-Sapphirine-Quartz Bearing Composite Inclusion Within Garnet From an Ultrahigh-Temperature Pelitic Granulite: Implications for Metamorphic History and P–T Path." *Lithos* 92: 524–536.

Uno, M., A. Okamoto, and N. Tsuchiya. 2017. "Excess Water Generation During Reaction-Inducing Intrusion of Granitic Melts Into Ultramafic Rocks at Crustal P–T Conditions in the Sør Rondane Mountains of East Antarctica." *Lithos* 284: 625–641.

Valley, J. W. 1986. "Stable Isotope Geochemistry of Metamorphic Rocks." In *Stable Isotopes in High Temperature Geological Processes*, edited by J. W. Valley, H. P. Taylor, and J. R. O'Neil, vol. 16, 445–490. Virginia: Mineralogical Society of America, Reviews in Mineralogy.

Valley, J. W., and J. R. O'Neil. 1981. "$^{13}C/^{12}C$ Exchange Between Calcite and Graphite a Possible Thermometer for Greenville Marbles." *Geochimica et Cosmochimica Acta* 45: 411–419.

Wada, H., N. Fujii, and N. Niitsuma. 1984. "Analytical Method of Stable Isotope for Ultra-Small Amounts of Carbon Dioxide With MAT-250 Mass Spectrometer." *Geoscience Reports of Shizuoka University* 10: 103–112.

Wada, H., and K. Suzuki. 1983. "Carbon Isotope Thermometry Calibrated by Dolomite-Calcite Solvus Temperatures." *Geochimica et Cosmochimica Acta* 47: 697–706.

Wada, H., T. Tomita, K. Matsuura, K. Iuchi, M. Ito, and T. Morikiyo. 1994. "Graphitisation of Carbonaceous Matter During Metamorphism With Reference to Carbonate and Pelitic Rocks of Contact and Regional Metamorphism, Japan." *Contributions to Mineralogy and Petrology* 118: 217–228.

Wang, C. C., J. Jacobs, M. A. Elburg, A. Läufer, and S. Elvevold. 2020. "Late Neoproterozoic–Cambrian Magmatism in Dronning Maud Land (East Antarctica): U–Pb Zircon Geochronology, Isotope Geochemistry and Implications for Gondwana Assembly." *Precambrian Research* 350: 105880.

Yoshimura, Y., Y. Motoyoshi, and T. Miyamoto. 2008. "Sapphirine + Quartz Association in Garnet: Implication for Ultrahigh-Temperature Metamorphism at Rundvågshetta, Lützow–Holm Complex, East Antarctica." In *Geodynamic Evolution of East Antarctica: A Key to the East-West Gondwana Connection*, edited by M. Satish-Kumar, Y. Motoyoshi, Y. Osanai, Y. Hiroi, and K. Shiraishi, vol. 308, 377–390. London: Geological Society of London, Special Publication.

Yuhara, M., A. Kamei, Y. Kawano, M. Owada, T. Shimura, and K. Tsukada. 2023. "High-K Adakitic Granite in Post-Gondwana Collisional Stage: Example for the Vengen Granite, Sør Rondane Mountains, East Antarctica." *Journal of Mineralogical and Petrological Sciences* 118: S010.